A Separation-Based Methodology to Consensus Tracking of Switched High-Order Nonlinear Multiagent Systems

Lv, Maolong; Yu, Wenwu; Cao, Jinde; Baldi, Simone

DOI
10.1109/TNNLS.2021.3070824

Publication date
2022

Document Version
Final published version

Published in
IEEE Transactions on Neural Networks and Learning Systems

A Separation-Based Methodology to Consensus Tracking of Switched High-Order Nonlinear Multiagent Systems

Maolong Lv, Wenwu Yu, *Senior Member, IEEE*, Jinde Cao, *Fellow, IEEE*, and Simone Baldi, *Senior Member, IEEE*

***Abstract*— This work investigates a reduced-complexity adaptive methodology to consensus tracking for a team of uncertain high-order nonlinear systems with switched (possibly asynchronous) dynamics. It is well known that high-order nonlinear systems are intrinsically challenging as feedback linearization and backstepping methods successfully developed for low-order systems fail to work. Even the adding-one-power-integrator methodology, well explored for the single-agent high-order case, presents some complexity issues and is unsuited for distributed control. At the core of the proposed distributed methodology is a newly proposed definition for separable functions: this definition allows the formulation of a separation-based lemma to handle the high-order terms with reduced complexity in the control design. Complexity is reduced in a twofold sense: the control gain of each virtual control law does not have to be incorporated in the next virtual control law iteratively, thus leading to a simpler expression of the control laws; the power of the virtual and actual control laws increases only proportionally (rather than exponentially) with the order of the systems, dramatically reducing high-gain issues.**

***Index Terms*— Consensus tracking, high-order nonlinear systems, multiagent systems, switching dynamics.**

I. Introduction

DISTRIBUTED leaderless or leader-following consensus control of nonlinear multiagent systems is more challenging but also potentially more applicable than its linear counterpart. Similar to the linear case, the goal is to steer a team of agents to a not globally known trajectory using only locally available information collected from neighboring agents [1]–[4]. In recent years, leaderless or leader-following consensus results have been obtained for two large families of nonlinear multiagent systems: strict-feedback [5]–[21] and pure-feedback multiagent systems [22]–[25]. For these families, the commonly adopted approach is an extension of the well-known backstepping technique [26] in a distributed sense. When the nonlinear functions are unknown, approximators such as neural networks and fuzzy logic systems have been incorporated in such a design. Switching dynamics can also be handled via the common Lyapunov function method [9], [23], [25]. Although strict-feedback and pure-feedback systems are popular dynamics in the nonlinear control field, there exist extensions to these dynamics: most notably, high-order nonlinear systems are a generalization of strict-feedback or pure-feedback systems since integrators with positive odd powers can appear in the dynamics (chain of positive odd power integrators). Literature has shown that high-order dynamics, appearing in aerospace and robotic applications [27]–[35], are extremely challenging to deal with, as their linearized dynamics might possess uncontrollable modes whose eigenvalues are on the right half-plane [36], making all standard feedback linearization or standard backstepping methodologies [6]–[10], [13]–[25], [37]–[39] fail for high-order systems [36]. Let us remark that the term "high-order" used in [27]–[33] (and in this work) is different than the term "high-order" used in [13], [14], [16], and [17]: the former term is often used in the nonlinear control community to indicate that the integrators in the chain may not only have power equal to one (low-order dynamics), but higher or equal to one (high-order dynamics); the latter term is often used in the consensus community to indicate that the chain is not composed by one linear integrator with power equal to one (first-order agents), nor by two linear integrators (second-order agents), but by more than two linear integrators (high-order agents). Therefore, from the point of view of [27]–[33], the dynamics of [13], [14], [16], [17] are strict-feedback and in fact standard backstepping techniques have been successfully adopted there. On the other hand, this work deals with "high-order" dynamics in the sense of [27]–[33], for which no standard backstepping technique can be adopted.

In place of the standard backstepping, the adding-one-power-integrator technique was successfully proposed in [28]

Manuscript received 4 May 2020; revised 24 October 2020; accepted 22 March 2021. Date of publication 14 April 2021; date of current version 6 October 2022. This work was supported in part by the Natural Science Foundation of China under Grant 61833005, Grant 61673107, and Grant 62073076; in part by the Double Innovation Plan under Grant 4207012004; in part by the Special Funding for Overseas talents under Grant 6207011901; and in part by the National Key Research and Development Project of China under Grant 2020YFA0714301. *(Corresponding author: Simone Baldi.)*

Maolong Lv is with the Delft Center for Systems and Control, Delft University of Technology, 2628 Delft, The Netherlands (e-mail: m.lyu@tudelft.nl).

Wenwu Yu is with the School of Mathematics, Southeast University, Nanjing 210096, China, and also with the Department of Electrical Engineering, Nantong University, Nantong 226019, China (e-mail: wwyu@seu.edu.cn).

Jinde Cao is with the School of Mathematics, Southeast University, Nanjing 210096, China, and also with the Yonsei Frontier Laboratory, Yonsei University, Seoul 03722, South Korea (e-mail: jdcao@seu.edu.cn).

Simone Baldi is with the School of Mathematics, Southeast University, Nanjing 210096, China, and also with the Delft Center for Systems and Control, Delft University of Technology, 2628 Delft, The Netherlands (e-mail: s.baldi@tudelft.nl).

Color versions of one or more figures in this article are available at https://doi.org/10.1109/TNNLS.2021.3070824.

Digital Object Identifier 10.1109/TNNLS.2021.3070824

to handle high-order dynamics. Progress made for the single high-order system case include relaxing the growth condition on the nonlinear functions [29], [30], [36] and employing neural network or fuzzy logic approximators to handle completely unknown nonlinearities [31]–[33], [40]. However, it has to be emphasized that a direct extension of the standard adding-one-power-integrator technique in a distributed sense is not meaningful due to some complex aspects of the procedure. At least the following two complex aspects are worth mentioning: 1) the high-power terms are separated from the control gain functions via *separation lemmas* that make the power of the virtual control gains grow exponentially with the power of the system; 2) the control gain of each virtual control is incorporated into the next virtual control law iteratively, thus increasing the control complexity at each step. Such issues result in high-complexity and high-gain designs which might be prohibitive for multiagent systems with low computational power and limited actuation. Therefore, the crucial open question motivating this research is: *how can reduced-complexity distributed methodologies be designed for high-order nonlinear multiagent systems?*

The main contribution of this work is to answer this question for a large class of uncertain high-order nonlinear multiagent systems, which can exhibit heterogeneous nonlinearities and switched dynamics with possibly asynchronous switches among the agents. At the core of the proposed methodology is a newly proposed definition for separable functions and a new separation-based lemma to deal with the high-power terms. The lemma decreases the aforementioned complex aspects of the state of the art in a twofold direction: 1) it avoids incorporating the control gain of each virtual control in the next virtual control law, thus sensibly reducing the complexity of the control action; 2) it allows the power of the virtual and actual control laws to increase only proportionally (rather than exponentially) with the order of the systems, thus dramatically reducing any high-gain issue (cf. the discussions in Remark 4 and 5 of this manuscript).

Notations: The notations adopted in this article are standard: $\mathbf{R}$ and $\mathbf{R}^n$ denote the set of real numbers and the n-dimensional Euclidean space, respectively. Q_{odd} represents the set of positive odd integers. $\|\cdot\|_2$ refers to either the Euclidean vector norm or the induced matrix 2-norm. For compactness and whenever unambiguous, throughout this article, some variable dependencies might be dropped, e.g., ξ, $h^j_{i,k}$, $\ell_{i,k}$, and $\upsilon_{i,k}$ can be used to denote $\xi(x_1, x_2)$, $h^j_{i,k}(\overline{\boldsymbol{x}}_{i,k})$, $\ell_{i,k}(s_{i,k+1}, \upsilon_{i,k})$, and $\upsilon_{i,k}(s_{i,k+1}, \upsilon_{i,k})$, respectively.

II. Problem Formulation and Preliminaries

Let us first give some preliminaries on graph theory. The communication topology is described by a directed graph $\mathscr{G} \triangleq (\mathscr{V}, \mathscr{E})$, with $\mathscr{V} \triangleq \{0, 1, \dots, N\}$ being the set of nodes (agents) and with $\mathscr{E} \subseteq \mathscr{V} \times \mathscr{V}$ being the set of directed edges between two distinct agents (self-edges are not allowed). A directed edge $(j, i) \in \mathscr{E}$ represents that agent i can obtain information from agent j. The neighbor set of agent i is denoted by $\mathscr{N}_i = \{j | (j, i) \in \mathscr{E}\}$: this is the set of agents from which agent i can obtain information. We reserve index 0 to the so-called leader agent: because agent 0 plays a special role, let us consider the subgraph defined by $\overline{\mathscr{G}} \triangleq (\overline{\mathscr{V}}, \overline{\mathscr{E}})$ with $\overline{\mathscr{V}} \triangleq \{1, 2, \dots, N\}$ and $\overline{\mathscr{E}}$ defined accordingly. For this subgraph, let us define the connectivity matrix $\overline{\mathscr{A}} = [a_{ij}] \in \mathbf{R}^{N\times N}$: if $(j, i)_{i\neq j} \in \overline{\mathscr{E}}$, then $a_{ij} = 1$, otherwise $a_{ij} = 0$ (note that $a_{ii} = 0$). The Laplacian matrix $\mathscr{L}$ associated with $\mathscr{G}$ is defined as

$$\mathscr{L} = \begin{bmatrix} 0 & \mathbf{0}_{1\times N} \\ -\boldsymbol{\mu} & \overline{\mathscr{L}} + \mathscr{B} \end{bmatrix}$$

with $\boldsymbol{\mu} = [\mu_1, \dots, \mu_N]^{\mathrm{T}}$, being $\mu_i = 1$ if the leader $0 \in \mathscr{N}_i$, and $\mu_i = 0$ otherwise. Also, $\mathscr{B} = \operatorname{diag}[\mu_1, \dots, \mu_N]^T$ and $\overline{\mathscr{L}} = \overline{\mathscr{D}} - \overline{\mathscr{A}}$ is the Laplacian matrix related to $\overline{\mathscr{G}}$ with $\overline{\mathscr{D}} = \operatorname{diag}[d_1, \dots, d_N]$, where $d_i = \sum_{j\in\mathscr{N}_i} a_{ij}$.

Consider a team of N ($N \geq 2$) switched high-order nonlinear multiagent systems whose dynamics are given by

$$\begin{cases} \dot{x}_{i,k} = \varphi^{\sigma_i(t)}_{i,k}(\overline{\boldsymbol{x}}_{i,k}) + h^{\sigma_i(t)}_{i,k}(\overline{\boldsymbol{x}}_{i,k}) x^{r_{i,k}}_{i,k+1}, \\ \dot{x}_{i,n_i} = \varphi^{\sigma_i(t)}_{i,n_i}(\overline{\boldsymbol{x}}_{i,n_i}) + h^{\sigma_i(t)}_{i,n_i}(\overline{\boldsymbol{x}}_{i,n_i}) u^{r_{i,n_i}}_i \\ y_i = x_{i,1} \end{cases} \tag{1}$$

with $1 \leq i \leq N$, $1 \leq k \leq n_i - 1$, $\overline{\boldsymbol{x}}_{i,k} = [x_{i,1}, \dots, x_{i,k}]^T \in \mathbf{R}^k$. The subscript i stands for "follower", to distinguish them from the leader agent, as clarified later. In (1), $\sigma_i(\cdot)$: $[0, +\infty) \to \mathscr{M}_i = \{1, 2, \dots, m_i\}$ is the switching signal for the ith follower, with $\mathscr{M}_i$ denoting the switching mode set and m_i denoting the number of modes for the ith follower; $r_{i,k} \in Q_{\text{odd}}$ are the high powers (positive odd integers), and $u^j_i \in \mathbf{R}$ is the control input for the jth mode of the ith follower. For each mode $\sigma_i(t)$, the functions $\varphi^{\sigma_i(t)}_{i,k}(\cdot)$ and $h^{\sigma_i(t)}_{i,k}(\cdot)$ are unknown continuous functions (for simplicity, we do not consider explicit time dependence in the nonlinear functions). The following remarks highlight the difference between (1) and other multiagent system models considered in literature.

Remark 1: (novelty and challenges of the class) The multiagent models in [6]–[10], [13]–[21] are strict-feedback low-order, i.e., special cases of (1) when all the powers $r_{i,k}$ are equal to one. Apart from this, (1) also possesses several levels of heterogeneity because: each follower agent exhibits its own switching $\sigma_i(\cdot)$, leading to possible asynchronous switching among the N followers; the unknown switched nonlinearities $\varphi^{\sigma_i(t)}_{i,k}(\cdot)$ and $h^{\sigma_i(t)}_{i,k}(\cdot)$ are possibly different for each follower. While similar levels of heterogeneity are considered in the pure-feedback multiagent models in [22]–[25], those multiagent systems models are also homologous to the strict-feedback low-order case, i.e. they can be equivalently transformed into the strict-feedback low-order form using the mean-value theorem.

Remark 2: (relevance of high-order nonlinear dynamics) High-order nonlinear dynamics have both mathematical and engineering relevance: from a mathematical point of view, standard feedback linearization and backstepping methods do not work for (1) due to the fact that the linearized dynamics may have uncontrollable modes (cf. discussions in [28] and [36]). From an engineering point of view, dynamics (1) can describe a large class of underactuated, weakly coupled, mechanical systems as shown in [36] and [41]. A practical example in this sense is also given in Section V-B. It is worth noting that, in line with [29], [36], [41], $r_{i,k}$ are odd integers since stabilization is not possible in general in the presence of even powers. This is because no matter if the virtual or actual control signals are positive or negative, they would become positive as per effect of the even power.

To facilitate distributed control design for (1), the following standard assumptions are made.

Assumption 1: [23] The leader agent 0 is represented by a leader output signal y_r, which is continuously differentiable, bounded, and available only to a subset of the follower agents. Furthermore, $\dot{y}_r$ is bounded and not available to any follower agent. The bounds for y_r and $\dot{y}_r$ are unknown.

Assumption 2: [19] The directed graph $\mathscr{G} = (\mathscr{V}, \mathscr{E})$ representing the multiagent communication contains at least one directed spanning tree with the leader agent as the root.

Assumption 3: [33] For each follower agent i, we assume the sign of $h^j_{i,k}$ is positive and there exist known real positive constants $\overline{h}^j_{i,k}$ and $\underline{h}^j_{i,k}$, $(1 \le k \le n_i,\ j \in \mathcal{M}_i)$ such that $\underline{h}^j_{i,k} \le h^j_{i,k}(\cdot) \le \overline{h}^j_{i,k}$.

Remark 3: (meaning of assumptions) Assumption 1 implies that the leader information is only available to a small fraction of followers. Assumption 2 implies that $\overline{\mathscr{L}+\mathscr{B}}$ is a nonsingular $\mathcal{M}$-matrix[1] and guarantees the feasibility of consensus [42]. Assumption 3 is a general controllability condition for many classes of nonlinear dynamics, including strict-feedback, pure-feedback, and high-order nonlinear systems [31]–[33].

A. Technical Lemmas

The following lemmas are useful for deriving the main results.

Lemma 1: [29] For any $x_1 \in \mathbf{R}$ and $x_2 \in \mathbf{R}$, and given positive integers b_1, b_2, and any real-valued function $\xi(x_1, x_2) > 0$, it holds that

$$|x_1|^{b_1}|x_2|^{b_2} \le \frac{b_1\xi|x_1|^{b_1+b_2}}{b_1+b_2} + \frac{b_2\xi^{-\frac{b_1}{b_2}}|x_2|^{b_1+b_2}}{b_1+b_2}. \tag{2}$$

Lemma 2: [33] Let x_1 and x_2 be real-valued functions. There exist a positive odd integer $\bar{h}$ and a constant $\bar{\lambda} \ge 1$ such that

$$\left|x_1^{\bar{h}} - x_2^{\bar{h}}\right| \le \bar{h}\left|x_1 - x_2\right|\left|x_1^{\bar{h}-1} + x_2^{\bar{h}-1}\right| \tag{3a}$$

$$|x_1 + x_2|^{\bar{\lambda}} \le 2^{\bar{\lambda}-1}\left(|x_1|^{\bar{\lambda}} + |x_2|^{\bar{\lambda}}\right). \tag{3b}$$

The following definition, lemma, and proposition are introduced to the purpose of reduced-complexity control, as it will be remarked later (cf. Remarks 4 and 5).

Definition 1: For any $x_1 \in \mathbf{R}$, $x_2 \in \mathbf{R}$, the continuous function $\digamma(\cdot)$: $\mathbf{R} \to \mathbf{R}$ is said to be a *separable function* provided that the following is satisfied:

$$\digamma(x_1 + x_2) = \ell(x_1, x_2)\digamma(x_1) + \upsilon(x_1, x_2)\digamma(x_2) \tag{4}$$

where $\ell(x_1, x_2) \in \left[\underline{\ell}_1, \overline{\ell}_1\right]$ with $\underline{\ell}_1 = 1-d$ and $\overline{\ell}_1 = 1+d$, with d an arbitrary constant taking value in $(0, 1)$, $|\upsilon(x_1, x_2)| \le \overline{\upsilon}(d)$ with $\overline{\upsilon}(d)$ denoting a positive continuous function that is independent of x_1 and x_2. Moreover, for a given d, value of $\overline{\upsilon}(d)$ is independent of x_1 and x_2.

[1] An $\mathcal{M}$-matrix is a square matrix with nonpositive off-diagonal entries and nonnegative principal minors.

Proposition 1: For any $x_1 \in \mathbf{R}$, $x_2 \in \mathbf{R}$, the continuous function $\digamma(\cdot)$ is a separable function if the following hold:
1) $\digamma(x_1x_2) = \digamma(x_1)\digamma(x_2)$
2) For $p \in \mathbf{R}$ and any constant d taking value in $(0, 1)$, a positive continuous function $\overline{\upsilon}(d)$ exists satisfying $|\digamma(\overline{p}) - 1| \le \overline{\upsilon}(d)|\digamma(p)| + d$, where $\overline{p} = p + 1$.

Proof: See Appendix.

Again, the linear function $\digamma(z) = z$ is a separable function since (1), (2) hold with $\overline{\upsilon}(d) = 1$ and any $0 < d < 1$. The following lemma states that any positive odd power function is a separable function.

Lemma 3: A function $\digamma(z) = z^r$ with r being a positive odd integer is a separable function. In particular, if we let $z = x_1 + x_2$, then, it holds that $(x_1 + x_2)^r = \ell(x_1, x_2)x_1^r + \upsilon(x_1, x_2)x_2^r$, where $\ell(x_1, x_2) \in \left[\underline{\ell}_1, \overline{\ell}_1\right]$ with $\underline{\ell}_1 = 1 - d$ and $\overline{\ell}_1 = 1 + d$, where $d = \sum_{k=1}^{r}(r!/k!(r-k)!)(r - k/r)l^{(r/r-k)}$ is an arbitrary constant taking value in $(0, 1)$ for some appropriately small constant l, $|\upsilon(x_1, x_2)| \le \overline{\upsilon}(d) = \sum_{k=1}^{r}(r!/k!(r-k)!)(k/r)l^{-(r/k)}$ with $\overline{\upsilon}(d)$ being a positive constant.

Proof: See Appendix.

B. Consensus Problem

Define the tracking error for the ith follower as:

$$s_{i,1} = \sum_{l\in\mathcal{N}_i} a_{il}(y_i - y_l) + \mu_i(y_i - y_r) \tag{5}$$

where $i = 1, \ldots, N$. After defining $\boldsymbol{s}_1 = [s_{1,1}, \ldots, s_{N,1}]^T \in \mathbf{R}^N$, one has $\boldsymbol{s}_1 = (\overline{\mathscr{L}+\mathscr{B}})\boldsymbol{\delta}$ where $\boldsymbol{\delta} = \bar{\boldsymbol{y}} - \bar{\boldsymbol{y}}_r$ with $\bar{\boldsymbol{y}} = [y_1, \ldots, y_N]^T$ and $\bar{\boldsymbol{y}}_r = [y_r, \ldots, y_r]^T$. Due to the nonsingularity of $\overline{\mathscr{L}+\mathscr{B}}$, it holds that $\|\boldsymbol{\delta}\|_2 \le (\|\boldsymbol{s}_1\|/\underline{\lambda}_{\min}(\overline{\mathscr{L}+\mathscr{B}}))$ [42], being $\underline{\lambda}_{\min}$ the minimum singular value of $\overline{\mathscr{L}+\mathscr{B}}$.

III. Proposed Distributed Consensus Design

Let us define the following variables for the ith follower:

$$s_{i,k} = x_{i,k} - \upsilon_{i,k-1}, \quad k = 2, \ldots, n_i \tag{6}$$

and let us propose the following design, whose rationale will be given in Section III-A:

$$\upsilon_{i,1} = -s_{i,1}\underbrace{R_{i,1}^{\frac{1}{r_{i,1}}}\left(c_{i,1} + \zeta_{i,1}^{\overline{r}_{i,1}}\widehat{\Xi}_{i,1}\Theta_{i,1}^{\overline{r}_{i,1}} + b_{i,1}^{\overline{r}_{i,1}}\right)^{\frac{1}{r_{i,1}}}}_{\varsigma_{i,1}} \tag{7}$$

$$R_{i,1} = \left[\underline{h}_{i,1}(d_i + \mu_i)(1-d)\right]^{-1} \tag{8}$$

$$\upsilon_{i,k} = -s_{i,k}\underbrace{R_{i,k}^{\frac{1}{r_{i,k}}}\left(c_{i,k} + \zeta_{i,k}^{\overline{r}_{i,k}}\widehat{\Xi}_{i,k}\Theta_{i,k}^{\overline{r}_{i,k}} + b_{i,k}^{\overline{r}_{i,k}}\right)^{\frac{1}{r_{i,k}}}}_{\varsigma_{i,k}} \tag{9}$$

$$R_{i,k} = \left[\underline{h}_{i,k}(1-d)\right]^{-1}, \ (k = 2, \ldots, n_i) \tag{10}$$

$$u_i \triangleq u_i^j = \upsilon_{i,n_i}, \quad j \in \mathcal{M}_i \tag{11}$$

where $r_i = \max_{1\le k\le n_i}\{r_{i,k}\}$, $\overline{r}_{i,k} = (r_i + 1/r_i - r_{i,k} + 1)$, $\underline{r}_{i,k} = (r_i + 1/r_{i,k})$, $\underline{h}_{i,k} = \min\left\{\underline{h}^j_{i,k}, j \in \mathcal{M}_i\right\}$, $\zeta_{i,k} > 0$, $b_{i,k} > 0$ and $c_{i,k} > 0$, $(k = 1, \ldots, n_i)$ are design constants.

Further, the parameters $\widehat{\Xi}_{i,k}$, $k = 1, \ldots, n_i$, are adapted via the laws

$$\dot{\widehat{\Xi}}_{i,k} = \beta_{i,k}\zeta_{i,k}^{\overline{r}_{i,k}}s_{i,k}^{r_i+1}\Theta_{i,k}^{\overline{r}_{i,k}} - \beta_{i,k}\sigma_{i,k}\widehat{\Xi}_{i,k} \tag{12}$$

where $\beta_{i,k} > 0$ denotes a tuning rate, $\sigma_{i,k} > 0$ stems from the leakage or σ-modification, well studied in robust adaptive control [43], and $\Theta_{i,k} > 0$ is a constant satisfying $\Theta_{i,k} \geq ||\boldsymbol{\phi}_{i,k}||$ according to [32, Lemma 3] with $\boldsymbol{\phi}_{i,k}$ being the activation functions coming from the use of radial basis function neural network (RBF NN) approximators [31]–[33]. The leakage or σ-modification is required to counteract the effect of disturbances or RBF NN approximation errors.

In the following, we describe the design steps leading to (7)–(12).

A. Design Steps

Step $i, 1$ ($i = 1, \ldots, N$): The time derivative of $s_{i,1}$ along (1) and (5) is

$$\dot{s}_{i,1} = (d_i + \mu_i) h_{i,1}^j(x_{i,1}) x_{i,2}^{r_{i,1}} + H_{i,1}^j \tag{13}$$

where $H_{i,1}^j$ is a function defined as

$$H_{i,1}^j = (d_i + \mu_i)\varphi_{i,1}^j(x_{i,1}) - \sum_{l \in \mathcal{N}_i} a_{il}\left(\varphi_{l,1}^j(x_{l,1}) + h_{l,1}^j(x_{l,1}) x_{l,2}^{r_{l,1}}\right) - \mu_i \dot{y}_r(t). \tag{14}$$

From Assumptions 1 and 3, and along similar ideas to [23], [33], [44], one can conclude that there exist a continuous function $F_{i,1}(\mathbf{Z}_{i,1})$ and a RBF NN approximator $\widehat{F}_{i,1}(\mathbf{Z}_{i,1}|\mathbf{W}_{i,1}^*)$ such that, for any $j \in \mathcal{M}_i$

$$\begin{aligned} s_{i,1}^{r_i - r_{i,1}+1} H_{i,1}^j &\leq \left|s_{i,1}^{r_i - r_{i,1}+1}\right| F_{i,1}(\mathbf{Z}_{i,1}) + \epsilon_{i,1} \\ &= \left|s_{i,1}^{r_i - r_{i,1}+1}\right| \left[\widehat{F}_{i,1}(\mathbf{Z}_{i,1}|\mathbf{W}_{i,1}^*) + \varepsilon_{i,1}(\mathbf{Z}_{i,1})\right] + \epsilon_{i,1} \\ &= \left|s_{i,1}^{r_i - r_{i,1}+1}\right| \left[\mathbf{W}_{i,1}^* \boldsymbol{\phi}_{i,1}(\mathbf{Z}_{i,1}) + \varepsilon_{i,1}(\mathbf{Z}_{i,1})\right] + \epsilon_{i,1} \end{aligned} \tag{15}$$

where $\mathbf{Z}_{i,1} = [x_{i,1}, x_{l,1,l\in\mathcal{N}_i}, x_{l,2,l\in\mathcal{N}_i}]^T$, $F_{i,1} = \max\{|H_{i,1}^j|, j \in \mathcal{M}_i\}$, $\epsilon_{i,1} > 0$ is a constant and $\varepsilon_{i,1}(\mathbf{Z}_{i,1})$ is the approximation error satisfying $|\varepsilon_{i,1}(\mathbf{Z}_{i,1})| \leq \overline{\varepsilon}_{i,1}$ on a compact set $\mathbf{\Omega}_{i,1}$, with $\mathbf{Z}_{i,1} \in \mathbf{\Omega}_{i,1}$ and $\overline{\varepsilon}_{i,1} > 0$ being a constant. The weight $\mathbf{W}_{i,1}^*$ is the optimal weight vector such that $\mathbf{W}_{i,1}^* = \arg\min_{\widehat{\mathbf{W}}_{i,1}^*} g\{\sup_{\Omega_{\mathbf{Z}_{i,1}}} |\widehat{F}_{i,1}(\mathbf{Z}_{i,1}|\widehat{\mathbf{W}}_{i,1}^*) - F_{i,1}(\mathbf{Z}_{i,1})| g\}$, with $\widehat{\mathbf{W}}_{i,1}^*$ being an estimate of $\mathbf{W}_{i,1}^*$. For subsequent analysis, let us define $\Xi_{i,1} = \|\mathbf{W}_{i,1}^*\|^{\overline{r}_{i,1}}$.

Consider the common Lyapunov function candidate

$$V_{i,1} = \frac{s_{i,1}^{r_i - r_{i,1}+2}}{r_i - r_{i,1} + 2} + \frac{1}{2\beta_{i,1}} \widetilde{\Xi}_{i,1}^2 \tag{16}$$

where $\widetilde{\Xi}_{i,1} = \Xi_{i,1} - \widehat{\Xi}_{i,1}$. Using Lemma 1 yields

$$\begin{aligned} \left|s_{i,1}^{r_i - r_{i,1}+1}\right| F_{i,1} &\leq \left|s_{i,1}^{r_i - r_{i,1}+1}\right| \left(\|\mathbf{W}_{i,1}^*\| \|\boldsymbol{\phi}_{i,1}\| + \overline{\varepsilon}_{i,1}\right) \\ &\leq \frac{1}{\underline{r}_{i,1}} \zeta_{i,1}^{-\underline{r}_{i,1}} + \frac{1}{\overline{r}_{i,1}} \zeta_{i,1}^{\overline{r}_{i,1}} s_{i,1}^{r_i+1} \left(\|\mathbf{W}_{i,1}^*\| \|\boldsymbol{\phi}_{i,1}\|\right)^{\overline{r}_{i,1}} \\ &\quad + \frac{1}{\overline{r}_{i,1}} b_{i,1}^{\overline{r}_{i,1}} s_{i,1}^{r_i+1} + \frac{1}{\underline{r}_{i,1}} b_{i,1}^{-\underline{r}_{i,1}} \overline{\varepsilon}_{i,1}^{\,\underline{r}_{i,1}} \\ &\leq s_{i,1}^{r_i+1}\left(b_{i,1}^{\overline{r}_{i,1}} + \zeta_{i,1}^{\overline{r}_{i,1}} \Xi_{i,1} \Theta_{i,1}^{\overline{r}_{i,1}}\right) + \kappa_{i,1} \end{aligned} \tag{17}$$

where the last inequality used the fact that $(1/\underline{r}_{i,1}) \leq 1$ and $||\boldsymbol{\phi}_{i,1}|| \leq \Theta_{i,1}$, $\kappa_{i,1} = \zeta_{i,1}^{-\underline{r}_{i,1}} + b_{i,1}^{-\underline{r}_{i,1}} \overline{\varepsilon}_{i,1}^{\,\underline{r}_{i,1}}$ with $\zeta_{i,1} > 0$ and $b_{i,1} > 0$ being design constants.

In light of (13), (14), and (16), the derivative of $V_{i,1}$ satisfies

$$\dot{V}_{i,1} \leq (d_i + \mu_i) s_{i,1}^{r_i - r_{i,1}+1} h_{i,1} x_{i,2}^{r_{i,1}} - \frac{\widetilde{\Xi}_{i,1} \dot{\widehat{\Xi}}_{i,1}}{\beta_{i,1}} + s_{i,1}^{r_i+1}\left(b_{i,1}^{\overline{r}_{i,1}} + \zeta_{i,1}^{\overline{r}_{i,1}} \Xi_{i,1} \Theta_{i,1}^{\overline{r}_{i,1}}\right) + \hbar_{i,1} \tag{18}$$

where $\hbar_{i,1} = \kappa_{i,1} + \epsilon_{i,1}$. We are now in the position to handle the term $x_{i,2}^{r_{i,1}}$ in (18) through the proposed Lemma 3 as

$$\begin{aligned} s_{i,1}^{r_i - r_{i,1}+1} x_{i,2}^{r_{i,1}} &= s_{i,1}^{r_i - r_{i,1}+1} (s_{i,2} + \upsilon_{i,1})^{r_{i,1}} \\ &\leq \overline{\upsilon}_{i,1} \left|s_{i,1}^{r_i - r_{i,1}+1} s_{i,2}^{r_{i,1}}\right| + s_{i,1}^{r_i - r_{i,1}+1} \ell_{i,1} \upsilon_{i,1}^{r_{i,1}}. \end{aligned} \tag{19}$$

Then, (18) can be rewritten as

$$\begin{aligned} \dot{V}_{i,1} \leq\ & (d_i + \mu_i) \overline{h}_{i,1}^j \overline{\upsilon}_{i,1} \left|s_{i,1}^{r_i - r_{i,1}+1} s_{i,2}^{r_{i,1}}\right| + (d_i + \mu_i) \\ & \times \left(h_{i,1}^j \ell_{i,1} s_{i,1}^{r_i - r_{i,1}+1} \upsilon_{i,1}^{r_{i,1}}\right) - \frac{1}{\beta_{i,1}} \widetilde{\Xi}_{i,1} \dot{\widehat{\Xi}}_{i,1} \\ & + s_{i,1}^{r_i+1}\left(b_{i,1}^{\overline{r}_{i,1}} + \zeta_{i,1}^{\overline{r}_{i,1}} \Xi_{i,1} \Theta_{i,1}^{\overline{r}_{i,1}}\right) + \hbar_{i,1}. \end{aligned} \tag{20}$$

Substituting the virtual controller $\upsilon_{i,1}$ (7) and the adaptation law $\dot{\widehat{\Xi}}_{i,1}$ (12) into (20), and using the fact that

$$\begin{aligned} \overline{h}_{i,1}^j \overline{\upsilon}_{i,1} \left|s_{i,1}^{r_i - r_{i,1}+1} s_{i,2}^{r_{i,1}}\right| &\leq \overline{\tau}_{i,1}\left(\frac{1}{\overline{r}_{i,1}} \rho_{i,1}^{\overline{r}_{i,1}} s_{i,1}^{r_i+1} + \frac{1}{\underline{r}_{i,1}} \varrho_{i,1}^{-\underline{r}_{i,1}} s_{i,2}^{r_i+1}\right) \\ &< \overline{\tau}_{i,1}\left(\rho_{i,1}^{\overline{r}_{i,1}} s_{i,1}^{r_i+1} + \varrho_{i,1}^{-\underline{r}_{i,1}} s_{i,2}^{r_i+1}\right) \end{aligned} \tag{21}$$

we can rewrite (20) as

$$\begin{aligned} \dot{V}_{i,1} &\leq -c_{i,1} s_{i,1}^{r_i+1} + (d_i + \mu_i) \overline{\tau}_{i,1} \rho_{i,1}^{\overline{r}_{i,1}} s_{i,1}^{r_i+1} + \hbar_{i,1} \\ &\quad + (d_i + \mu_i) \overline{\tau}_{i,1} \varrho_{i,1}^{-\underline{r}_{i,1}} s_{i,2}^{r_i+1} + \frac{1}{2}\sigma_{i,1} \widetilde{\Xi}_{i,1} \widehat{\Xi}_{i,1} \\ &\leq -(c_{i,1} - \theta_{i,1}) s_{i,1}^{r_i+1} + \vartheta_{i,1} s_{i,2}^{r_i+1} + \hbar_{i,1} \\ &\quad + \frac{1}{2}\sigma_{i,1} \Xi_{i,1}^2 - \frac{1}{2}\sigma_{i,1} \widetilde{\Xi}_{i,1}^2 \end{aligned} \tag{22}$$

where $\overline{\tau}_{i,1} = \overline{h}_{i,1}^j \overline{\upsilon}_{i,1}$, $\theta_{i,1} = (d_i + \mu_i) \overline{\tau}_{i,1} \rho_{i,1}^{\overline{r}_{i,1}}$ and $\vartheta_{i,1} = (d_i + \mu_i) \overline{\tau}_{i,1} \varrho_{i,1}^{-\underline{r}_{i,1}}$ with $\rho_{i,1} > 0$ and $\varrho_{i,1} > 0$ being design constants.

Step $i, 2$ ($i = 1, \ldots, N$): Taking the derivative of $s_{i,2}$ yields

$$\dot{s}_{i,2} = h_{i,2}^j(\overline{\mathbf{x}}_{i,2}) x_{i,3}^{r_{i,2}} + H_{i,2}^j \tag{23}$$

where $H_{i,2}^j$ is a function defined as

$$\begin{aligned} H_{i,2}^j = \varphi_{i,2}^j(\overline{\mathbf{x}}_{i,2}) &- \frac{\partial \upsilon_{i,1}}{\partial x_{i,1}}\left(\varphi_{i,1}^j(x_{i,1}) + h_{i,1}^j x_{i,2}^{r_{i,1}}\right) \\ &- \sum_{l \in \mathcal{N}_i} a_{il} \frac{\partial \upsilon_{i,1}}{\partial x_{l,1}}\left(\varphi_{l,1}^j(x_{l,1}) + h_{l,1}^j x_{l,2}^{r_{l,1}}\right) \\ &- \frac{\partial \upsilon_{i,1}}{\partial y_r} \dot{y}_r - \frac{\partial \upsilon_{i,1}}{\partial \widehat{\Xi}_{i,1}} \dot{\widehat{\Xi}}_{i,1}. \end{aligned} \tag{24}$$

Proceeding similar to Step $i, 1$, there exist a continuous function $F_{i,2}(\mathbf{Z}_{i,2})$ and a RBF NN approximator $\widehat{F}_{i,2}(\mathbf{Z}_{i,2}|\mathbf{W}_{i,2}^*)$

such that, for any $j \in \mathcal{M}_i$

$$\begin{aligned} s_{i,2}^{r_i - r_{i,2}+1} H_{i,2}^j &\le \left| s_{i,2}^{r_i - r_{i,2}+1} \right| F_{i,2}(\mathbf{Z}_{i,2}) + \epsilon_{i,2} \\ &= \left| s_{i,2}^{r_i - r_{i,2}+1} \right| \left[\widehat{F}_{i,2}\left(\mathbf{Z}_{i,2} \middle| \mathbf{W}_{i,2}^*\right) + \varepsilon_{i,2}(\mathbf{Z}_{i,2}) \right] + \epsilon_{i,2} \\ &= \left| s_{i,2}^{r_i - r_{i,2}+1} \right| \left[\mathbf{W}_{i,2}^* \boldsymbol{\phi}_{i,2}(\mathbf{Z}_{i,2}) + \varepsilon_{i,2}(\mathbf{Z}_{i,2}) \right] + \epsilon_{i,2} \end{aligned} \tag{25}$$

where $\mathbf{Z}_{i,2} = [\overline{\boldsymbol{x}}_{i,2}, \overline{\boldsymbol{x}}_{l,2,l\in\mathcal{N}_i}, (\partial v_{i,1}/\partial x_{l,1}), (\partial v_{i,1}/\partial x_{i,1}), (\partial v_{i,1}/\partial y_r), (\partial v_{i,1}/\partial \widehat{\Xi}_{i,1}), \widehat{\Xi}_{i,1}, y_r]^T$, $F_{i,2} = \max\{|H_{i,2}^j|,\ j \in \mathcal{M}_i\}$, $\epsilon_{i,2} > 0$ is a constant and $|\varepsilon_{i,2}(\mathbf{Z}_{i,2})| \le \overline{\varepsilon}_{i,2}$ with $\overline{\varepsilon}_{i,2} > 0$ being a constant. The optimal weight $\mathbf{W}_{i,2}^*$ and its estimate $\widehat{\mathbf{W}}_{i,2}^*$ are defined in a similar way as the previous step. Then, let us define $\Xi_{i,2} = \|\mathbf{W}_{i,2}^*\|^{\overline{r}_{i,2}}$.

Consider the common Lyapunov function candidate

$$V_{i,2} = V_{i,1} + \frac{s_{i,2}^{r_i - r_{i,2}+2}}{r_i - r_{i,2} + 2} + \frac{1}{2\beta_{i,2}} \widetilde{\Xi}_{i,2}^2 \tag{26}$$

where $\widetilde{\Xi}_{i,2} = \Xi_{i,2} - \widehat{\Xi}_{i,2}$. Along similar lines as (17), we obtain the following inequality:

$$\left| s_{i,2}^{r_i - r_{i,2}+1} \right| F_{i,2} \le s_{i,2}^{r_i+1} \left(b_{i,2}^{\overline{r}_{i,2}} + \zeta_{i,2}^{\overline{r}_{i,2}} \Xi_{i,2} \Theta_{i,2}^{\overline{r}_{i,2}} \right) + \kappa_{i,2} \tag{27}$$

where $\Theta_{i,2} \ge ||\boldsymbol{\phi}_{i,2}|| > 0$ is a constant, $\kappa_{i,2} = \zeta_{i,2}^{-\underline{r}_{i,2}} + b_{i,2}^{-\underline{r}_{i,2}} \overline{\varepsilon}_{i,2}^{\underline{r}_{i,2}}$ with $\zeta_{i,2} > 0$ and $b_{i,2} > 0$ being design constants. Hence, the derivative of $V_{i,2}$ along (22) and (23) is

$$\begin{aligned} \dot{V}_{i,2} \le & -(c_{i,1} - \theta_{i,1}) s_{i,1}^{r_i+1} + h_{i,2}^j(\overline{x}_{i,2}) s_{i,2}^{r_i - r_{i,2}+1} x_{i,3}^{r_{i,2}} \\ & - \frac{1}{\beta_{i,2}} \widetilde{\Xi}_{i,2} \dot{\widehat{\Xi}}_{i,2} + s_{i,2}^{r_i+1} \left(b_{i,2}^{\overline{r}_{i,2}} + \zeta_{i,2}^{\overline{r}_{i,2}} \Xi_{i,2} \Theta_{i,2}^{\overline{r}_{i,2}} \right) \\ & + \frac{\sigma_{i,1}}{2} \left(\Xi_{i,1}^2 - \widetilde{\Xi}_{i,1}^2 \right) + \vartheta_{i,1} s_{i,2}^{r_i+1} + \hbar_{i,1} + \hbar_{i,2} \end{aligned}$$

where $\hbar_{i,2} = \kappa_{i,2} + \epsilon_{i,2}$. Similar to (19), the use of the proposed Lemma 3 gives

$$\begin{aligned} s_{i,2}^{r_i - r_{i,2}+1} x_{i,3}^{r_{i,2}} &= s_{i,2}^{r_i - r_{i,2}+1} \left(s_{i,3} + v_{i,2}\right)^{r_{i,2}} \\ &\le \overline{v}_{f,2} \left| s_{i,2}^{r_i - r_{i,2}+1} s_{i,3}^{r_{i,2}} \right| + s_{i,2}^{r_i - r_{i,2}+1} \ell_{i,2} v_{i,2}^{r_{i,2}}. \end{aligned} \tag{28}$$

Remark 4: (departure from state-of-the-art designs) To highlight the distinguishing feature of the proposed design, let us recall the standard designs in [29], [31]–[33], [36], [40]. There, instead of (28), $x_{i,3}^{r_{i,2}}$ is tackled by subtracting and adding $v_{i,2}^{r_{i,2}}$, namely

$$s_{i,2}^{r_i - r_{i,2}+1} x_{i,3}^{r_{i,2}} = s_{i,2}^{r_i - r_{i,2}+1} \left[\left(x_{i,3}^{r_{i,2}} - v_{i,2}^{r_{i,2}} \right) + v_{i,2}^{r_{i,2}} \right].$$

Then, the use of Lemmas 1 and 2 yields

$$\begin{aligned} s_{i,2}^{r_i - r_{i,2}+1} \left(x_{i,3}^{r_{i,2}} - v_{i,2}^{r_{i,2}} \right) \le\ & r_{i,2} \left| s_{i,2}^{r_i - r_{i,2}+1} \right| |s_{i,3}| \\ & \left[2^{r_{i,2}-2} \left(s_{i,3}^{r_{i,2}-1} + v_{i,2}^{r_{i,2}-1} \right) \right. \\ & \left. + \left(s_{i,2} \varsigma_{i,2}\right)^{r_{i,2}-1} \right] \le s_{i,2}^{r_i+1} + \overline{\varsigma}_{i,2} s_{i,3}^{r_i+1} \end{aligned} \tag{29}$$

where $\overline{\varsigma}_{i,2} = \left(2^{r_{i,2}-2} r_{i,2}\right)^{\underline{r}_{i,2}} + \left(2^{r_{i,2}-2} r_{i,2} \varsigma_{i,2}^{r_{i,2}-1}\right)^{r_i+1}$. However, for the methods in [29], [31]–[33], [36], [40] to work, $\overline{\varsigma}_{i,2}$ is incorporated into the virtual control law $v_{i,3}$ to eliminate the extra term $\overline{\varsigma}_{i,2} s_{i,3}^{r_i+1}$ (e.g., [31, eq.(5)], [32, eq.(12)], [33, eq.(4)], [36, the equation after (3.11)]), [40, eq. (23)]: this inevitably increases the complexity of the controller structure. It is also worth remarking that the power of the control gain $\overline{\varsigma}_{i,k}$ in (29) grows dramatically (exponentially) as the order of the subsystems grows, leading to possibly high control gains. This is in contrast with the power of the control gain in (28) which is proportional to the power of the subsystems.

Remark 5: (effects of the separation lemma) The benefits brought by the proposed Lemma 3 can be summarized as: (i) in the first line of (28), the virtual control $v_{i,2}$ can be extracted from $\left(s_{i,3} + v_{i,2}\right)^{r_{i,2}-1}$ directly without involving any inequalities scaling as in ([31, eq.(17)], [32, eq.(29)], [33, eq.(20)], [36, eq.(3.8)]), [40, eq. (20)] implying that the term $\overline{\varsigma}_{i,2}$ will not appear; (ii) the term $v_{i,2}$ in (28) is eventually upper bounded by a constant $\overline{v}_{i,2}$, which is independent of $s_{i,3}$ and $v_{i,2}$, and can be easily handled as shown hereafter.

At this point, similar to (21), we can bound one of the terms in (28) as

$$\begin{aligned} \overline{h}_{i,2}^j \overline{v}_{i,2} \left| s_{i,2}^{r_i - r_{i,2}+1} \right| \left| s_{i,3}^{r_{i,2}} \right| &= \overline{\tau}_{i,2} \left| s_{i,2}^{r_i - r_{i,2}+1} \right| \left| s_{i,3}^{r_{i,2}} \right| \\ &\le \overline{\tau}_{i,2} \left(\rho_{i,2}^{\overline{r}_{i,2}} s_{i,2}^{r_i+1} + \varrho_{i,2}^{-\underline{r}_{i,2}} s_{i,3}^{r_i+1} \right) \end{aligned} \tag{30}$$

where $\overline{\tau}_{i,2} = \overline{h}_{i,2}^j \overline{v}_{i,2}$, $\rho_{i,2} > 0$ and $\varrho_{i,2} > 0$ are design constants.

Substituting the virtual controller $v_{i,2}$ in (9) and the adaptation law $\dot{\widehat{\Xi}}_{i,2}$ in (12) into the Lyapunov derivative after (27) results in

$$\begin{aligned} \dot{V}_{i,2} \le & -(c_{i,1} - \theta_{i,1}) s_{i,1}^{r_i+1} - (c_{i,2} - \vartheta_{i,1} - \theta_{i,2}) s_{i,2}^{r_i+1} \\ & + \vartheta_{i,2} s_{i,3}^{r_i+1} + \sum_{k=1}^{2} \left(\frac{\sigma_{i,k}}{2} \Xi_{i,k}^2 - \frac{\sigma_{i,k}}{2} \widetilde{\Xi}_{i,k}^2 + \hbar_{i,k} \right) \end{aligned}$$

where $\theta_{i,2} = \overline{\tau}_{i,2} \rho_{i,2}^{\overline{r}_{i,2}}$ and $\vartheta_{i,2} = \overline{\tau}_{i,2} \varrho_{i,2}^{-\underline{r}_{i,2}}$.

Step i, k ($i = 1, \ldots, N,\ k = 3, \ldots, n_i - 1$): It follows from (1) and (6) that the derivative of $s_{i,k}$ is:

$$\dot{s}_{i,k} = h_{i,k}^j(\overline{\boldsymbol{x}}_{i,k}) x_{i,k+1}^{r_{i,k}} + H_{i,k}^j \tag{31}$$

where $H_{i,k}^j$ is a function defined as

$$\begin{aligned} H_{i,k}^j = & \varphi_{i,k}^j(\overline{\boldsymbol{x}}_{i,k}) - \sum_{l\in\mathcal{N}_i} \frac{\partial v_{i,k-1}}{\partial x_{l,1}} \left(\varphi_{l,1}^j(x_{l,1}) + h_{l,1}^j x_{l,2}^{r_{l,1}} \right) \\ & - \sum_{q=1}^{k-1} \frac{\partial v_{i,k-1}}{\partial x_{i,q}} \left(\varphi_{i,q}^j(\overline{\boldsymbol{x}}_{i,q}) + h_{i,q}^j x_{i,q+1}^{r_{i,q}} \right) \\ & - \sum_{q=1}^{k-1} \frac{\partial v_{i,k-1}}{\partial \widehat{\Xi}_{i,q}} \dot{\widehat{\Xi}}_{i,q} - \frac{\partial v_{i,k-1}}{\partial y_r} \dot{y}_r. \end{aligned} \tag{32}$$

Likewise, there exist a continuous function $F_{i,k}\left(\mathbf{Z}_{i,k}\right)$ and a RBF NN approximator $\widehat{F}_{i,k}\left(\mathbf{Z}_{i,k} \middle| \mathbf{W}_{i,k}^*\right)$ such that, for any $j \in$

$\mathcal{M}_i$

$$\begin{aligned} s_{i,k}^{r_i-r_{i,k}+1}H_{i,k}^j &\le \left|s_{i,k}^{r_i-r_{i,k}+1}\right|F_{i,k}(\mathbf{Z}_{i,k})+\epsilon_{i,k} \\ &= \left|s_{i,k}^{r_i-r_{i,k}+1}\right|\Big[\widehat{F}_{i,k}\big(\mathbf{Z}_{i,k}\big|\mathbf{W}_{i,k}^*\big)+\varepsilon_{i,k}(\mathbf{Z}_{i,k})\Big]+\epsilon_{i,k} \\ &= \left|s_{i,k}^{r_i-r_{i,k}+1}\right|\Big[\mathbf{W}_{i,k}^*\boldsymbol{\phi}_{i,k}(\mathbf{Z}_{i,k})+\varepsilon_{i,k}(\mathbf{Z}_{i,k})\Big]+\epsilon_{i,k} \end{aligned} \tag{33}$$

where $\mathbf{Z}_{i,k} = [\overline{\mathbf{x}}_{i,k}, \overline{\mathbf{x}}_{l,2,l\in\mathcal{N}_i}, (\partial v_{i,k-1}/\partial x_{l,1}), (\partial v_{i,k-1}/\partial x_{i,1}), \ldots, (\partial v_{i,k-1}/\partial x_{i,k-1}), (\partial v_{i,k-1}/\partial\widehat{\Xi}_{i,1}), \ldots, (\partial v_{i,k-1}/\partial\widehat{\Xi}_{i,k-1}), \widehat{\Xi}_{i,1}, \ldots, \widehat{\Xi}_{i,k-1}, (\partial v_{i,k-1}/\partial y_r), y_r]^T$, $F_{i,k} = \max\{\,|H_{i,k}^j|, j\in\mathcal{M}_i\}$, $\epsilon_{i,k} > 0$ is a constant and $|\varepsilon_{i,k}(\mathbf{Z}_{i,k})| \le \overline{\varepsilon}_{i,k}$ with $\overline{\varepsilon}_{i,k} > 0$ being a constant. The optimal weight $\mathbf{W}_{i,k}^*$ and its estimate $\widehat{\mathbf{W}}_{i,k}^*$ are defined in a similar way as the previous steps. Let us further define $\Xi_{i,k} = \|\mathbf{W}_{i,k}^*\|^{\overline{r}_{i,k}}$.

Consider the common Lyapunov function candidate

$$V_{i,k} = V_{i,k-1} + \frac{s_{i,k}^{r_i-r_{i,k}+2}}{r_i - r_{i,k}+2} + \frac{1}{2\beta_{i,k}}\widetilde{\Xi}_{i,k}^2 \tag{34}$$

where $\widetilde{\Xi}_{i,k} = \Xi_{i,k} - \widehat{\Xi}_{i,k}$. Following similar lines as Step $i,1$ and Step $i,2$, it is possible to obtain the derivative of $V_{i,k}$ as:

$$\begin{aligned} \dot{V}_{i,k} \le &-\sum_{m=1}^{k}\big(c_{i,m}-\theta_{i,m}-\vartheta_{i,m-1}\big)s_{i,m}^{r_i+1} + \vartheta_{i,k}s_{i,k+1}^{r_i+1} \\ &+ \sum_{m=1}^{k}\left(\frac{\sigma_{i,m}}{2}\Xi_{i,m}^2 - \frac{\sigma_{i,m}}{2}\widetilde{\Xi}_{i,m}^2 + \hbar_{i,m}\right) \end{aligned} \tag{35}$$

where $\vartheta_{i,0} = 0$, $\theta_{i,1} = (d_i+\mu_i)\overline{\tau}_{i,1}\rho_{i,1}^{\overline{r}_{i,1}}$, $\vartheta_{i,1} = (d_i+\mu_i)\overline{\tau}_{i,1}\varrho_{i,1}^{-\underline{r}_{i,1}}$, $\theta_{i,m} = \overline{\tau}_{i,m}\rho_{i,m}^{\overline{r}_{i,m}}$ and $\vartheta_{i,m} = \overline{\tau}_{i,m}\varrho_{i,m}^{-\underline{r}_{i,m}} (m = 2,\ldots,k)$, $\overline{\tau}_{i,m} = \overline{h}_{i,m}^j\overline{v}_{i,m}$ with $\overline{v}_{i,m}$ being the upper bound of $v_{i,m}(s_{i,m+1}, v_{i,m})$, $\hbar_{i,m} = \kappa_{i,m}+\epsilon_{i,m}$, $\kappa_{i,m} = \zeta_{i,m}^{-\underline{r}_{i,m}} + b_{i,m}^{-\underline{r}_{i,m}}\overline{\varepsilon}_{i,m}^{\,\underline{r}_{i,m}}$, $\zeta_{i,m} > 0$, $b_{i,m} > 0$, $c_{i,m} > 0$, $\rho_{i,m} > 0$ and $\varrho_{i,m} > 0$ are design parameters.

Step i, n_i $(i = 1,\ldots,N)$: For the final step, the derivative of s_{i,n_i} along (1) and (6) is

$$\dot{s}_{i,n_i} = h_{i,n_i}^j(\overline{\mathbf{x}}_{i,n_i})u_i^{r_{i,n_i}} + H_{i,n_i}^j \tag{36}$$

where H_{i,n_i}^j is a function defined as

$$\begin{aligned} H_{i,n_i}^j = &\ \varphi_{i,n_i}^j(\overline{\mathbf{x}}_{i,n_i}) - \sum_{l\in\mathcal{N}_f}\frac{\partial v_{i,n_i-1}}{\partial x_{l,1}}\Big(\varphi_{l,1}^j(x_{l,1}) + h_{l,1}^j x_{l,2}^{r_{l,1}}\Big) \\ &- \sum_{q=1}^{n_i-1}\frac{\partial v_{i,n_i-1}}{\partial x_{i,q}}\Big(\varphi_{i,q}^j(\overline{\mathbf{x}}_{i,q}) + h_{i,q}^j x_{i,q+1}^{r_{i,q}}\Big) \\ &- \sum_{q=1}^{n_i-1}\frac{\partial v_{i,n_i-1}}{\partial\widehat{\Xi}_{i,q}}\dot{\widehat{\Xi}}_{i,q} - \frac{\partial v_{i,n_i-1}}{\partial y_r}\dot{y}_r. \end{aligned} \tag{37}$$

Similar to steps (15), (25), and (33), there exist a continuous function $F_{i,n_i}(\mathbf{Z}_{i,n_i})$ and a RBF NN approximator $\widehat{F}_{i,n_i}(\mathbf{Z}_{i,n_i}|\mathbf{W}_{i,n_i}^*)$ such that, for any $j\in\mathcal{M}_i$

$$\begin{aligned} s_{i,n_i}^{r_i-r_{i,n_i}+1}H_{i,n_i}^j &\le \left|s_{i,n_i}^{r_i-r_{i,n_i}+1}\right|F_{i,n_i}(\mathbf{Z}_{i,n_i})+\epsilon_{i,n_i} = \left|s_{i,n_i}^{r_i-r_{i,n_i}+1}\right| \\ &\quad\times\Big[\widehat{F}_{i,n_i}\big(\mathbf{Z}_{i,n_i}\big|\mathbf{W}_{i,n_i}^*\big)+\varepsilon_{i,n_i}(\mathbf{Z}_{i,n_i})\Big]+\epsilon_{i,n_i} \\ &= \left|s_{i,n_i}^{r_i-r_{i,n_i}+1}\right|\Big[\mathbf{W}_{i,n_i}^*\boldsymbol{\phi}_{i,n_i}(\mathbf{Z}_{i,n_i})+\varepsilon_{i,n_i}(\mathbf{Z}_{i,n_i})\Big] \\ &\quad+\epsilon_{i,n_i} \end{aligned} \tag{38}$$

where $\mathbf{Z}_{i,n_i} = [\overline{\mathbf{x}}_{i,n_i}, \overline{\mathbf{x}}_{l,2,l\in\mathcal{N}_i}, (\partial v_{i,n_i-1}/\partial x_{l,1}), (\partial v_{i,n_i-1}/\partial x_{i,1}), \ldots, (\partial v_{i,n_i-1}/\partial x_{i,n_i-1}), (\partial v_{i,n_i-1}/\partial\widehat{\Xi}_{i,1}), \ldots, (\partial v_{i,n_i-1}/\partial\widehat{\Xi}_{i,n_i-1}), \widehat{\Xi}_{i,1}, \ldots, \widehat{\Xi}_{i,n_i-1}, (\partial v_{i,n_i-1}/\partial y_r), y_r]^T$, $F_{i,n_i} = \max\{|H_{i,n_i}^j|,\ j\in\mathcal{M}_i\}$, $\epsilon_{i,n_i} > 0$ is a constant and $|\varepsilon_{i,n_i}(\mathbf{Z}_{i,n_i})| \le \overline{\varepsilon}_{i,n_i}$ with $\overline{\varepsilon}_{i,n_i} > 0$ being a constant. The optimal weight $\mathbf{W}_{i,n_i}^*$ and its estimate $\widehat{\mathbf{W}}_{i,n_i}^*$ are defined in a similar way as the previous steps. Let us further define $\Xi_{i,n_i} = \|\mathbf{W}_{i,n_i}^*\|^{\overline{r}_{i,n_i}}$.

Consider the common Lyapunov function candidate

$$V_{i,n_i} = V_{i,n_i-1} + \frac{s_{i,n_i}^{r_i-r_{i,n_i}+2}}{r_i-r_{i,n_i}+2} + \frac{1}{2\beta_{i,n_i}}\widetilde{\Xi}_{i,n_i}^2 \tag{39}$$

where $\widetilde{\Xi}_{i,n_i} = \Xi_{i,n_i} - \widehat{\Xi}_{i,n_i}$.

Choosing the common actual controller $u_i \triangleq u_i^j$ for the ith follower as (11), one immediately gets from (35) that:

$$\begin{aligned} \dot{V}_{i,n_i} \le &-\sum_{k=1}^{n_i}\big(c_{i,k}-\theta_{i,k}-\vartheta_{i,k-1}\big)\gamma_i^{\frac{r_{i,k}-1}{r_i+1}}s_{i,k}^{r_i-r_{i,k}+2} \\ &+\sum_{k=1}^{n_i}\left(\frac{1}{2}\sigma_{i,k}\Xi_{i,k}^2 - \frac{1}{2}\sigma_{i,k}\widetilde{\Xi}_{i,k}^2 + \hbar_{i,k}\right) \\ &+\sum_{k=1}^{n_i}\Big(\gamma_i\big(c_{i,k}-\theta_{i,k}-\vartheta_{i,k-1}\big)\Big) \end{aligned} \tag{40}$$

where above inequality holds due to $\vartheta_{i,0} = 0$, $s_{i,n_i+1} = 0$ and the fact that

$$\gamma_i^{(r_{i,n_i}-1)/(r_i+1)}s_{i,n_i}^{r_i-r_{i,n_i}+2} \le \gamma_i + s_{i,n_i}^{r_i+1} \tag{41}$$

with $\gamma_i > 0$ a constant, according to Lemma 1.

IV. Stability Analysis

To analyze the stability of the entire closed-loop system, consider the combined common Lyapunov function

$$V = \sum_{i=1}^{N} V_{i,n_i}. \tag{42}$$

The use of the common Lyapunov function (42) is possible because in (15), (25), (33), and (38), the maximum value of the switching weights is estimated by the RBF NN approximators. A multiple Lyapunov function approach is in principle possible, but in this case the stability analysis requires to impose conditions on the switching signal [43]. With the common Lyapunov function (42), the following stability result holds for arbitrary switching $\sigma_i(\cdot)$.

Theorem 1: Under Assumptions 1–3, consider the closed-loop system composed by the high-order switched nonlinear multiagent system (1), the distributed adaptive consensus controllers (7)–(11) and the parameter adaptation laws (12). For any $\varpi > 0$, and the initial conditions $\overline{\mathbf{x}}_{i,k}(0)$ and $\widehat{\Xi}_{i,k}(0)$ for $(i = 1,\ldots,N,\ k = 1,\ldots,n_i)$ satisfying $V(\overline{\mathbf{x}}_{i,k}(0), \widehat{\Xi}_{i,k}(0)) < \varpi$, there exist positive design parameters $c_{i,k}$, $\beta_{i,k}$, $\sigma_{i,k}$, $\zeta_{i,k}$, $b_{i,k}$, γ_i, $\rho_{i,k}$, $\varrho_{i,k}$, and $\Theta_{i,k}$, $i = 1,\ldots,N$, $k = 1,\ldots,n_i$, such that

1) *The compact set $\Omega_0 = \Big\{(\overline{\mathbf{x}}_{i,k}, \widehat{\Xi}_{i,k})|V(\overline{\mathbf{x}}_{i,k}, \widehat{\Xi}_{i,k}) \le \varpi, i = 1,\ldots,N, k = 1,\ldots,n_i\Big\}$ is an invariant set, namely, $V(\overline{\mathbf{x}}_{i,k}, \widehat{\Xi}_{i,k}) \le \varpi$ holds for $\forall t \ge 0$, and hence all the closed-loop signals are bounded all the time;*

2) *The consensus tracking error $\boldsymbol{\delta}$ converges to the following compact set:*

$$\Omega_3 = \left\{ \lim_{t\to+\infty} \|\boldsymbol{\delta}\|_2 \le \sqrt{\frac{\sum_{i=1}^{N}\left[\frac{\chi}{\overline{\alpha}}\overline{\psi}_i\right]^{\frac{2}{\underline{\psi}_i}}}{\lambda^2_{\min}\left(\mathscr{L}+\mathscr{B}\right)}} \triangleq \Psi \right\} \tag{43}$$

where $\overline{\psi}_i = \max\{r_i - r_{i,1} + 2, i \in \mathcal{M}_i\}$, $\underline{\psi}_i = \min\{r_i - r_{i,1} + 2, i \in \mathcal{M}_i\}$, $\overline{\alpha}$, *and* χ *are given in the proof.*

Proof: See Appendix.

In case the knowledge of $\underline{\lambda}_{\min}(\mathscr{L}+\mathscr{B})$ is not available, it was proposed to replace this terms in (43) with the more conservative bound $(\overline{N}/N^2+N-1)$ with $\overline{N} = ((N-1/N))^{(N-1/2)}$ [45].

A design procedure for the proposed algorithm can be sketched as follows:

Step 1: Specify a constant $\varpi > 0$ and choose appropriate initial conditions $x_{i,k}(0)$ and $\widehat{\Xi}_{i,k}(0) \ge 0$ for $i = 1,\ldots,N$, $k = 1,\ldots,n_i$ to satisfy $V(0) < \varpi$;

Step 2: Choose RBF NN approximators $\widehat{\boldsymbol{W}}_{i,k}\boldsymbol{\phi}_{i,k}(\boldsymbol{Z}_{i,k})$ by appropriately selecting the number of network nodes, where $i = 1,\ldots,N$, $k = 1,\ldots,n_i$. Accordingly, calculate $\Theta_{i,k}$.

Step 3: Assign specific values to the design parameters $c_{i,k} > 0$, $\sigma_{i,k} > 0$, $\beta_{i,k} > 0$, $\zeta_{i,k} > 0$, $\gamma_i > 0$, $b_{i,k} > 0$, $\rho_{i,k} > 0$, and $\varrho_{i,k} > 0$.

Step 4: Determine the intermediate variables according to the following order: $s_{i,1} \to \widehat{\Xi}_{i,1} \to \upsilon_{i,1} \to s_{i,2} \to \widehat{\Xi}_{i,2} \to \upsilon_{i,2} \to \cdots s_{i,k} \to \widehat{\Xi}_{i,k} \to \upsilon_{i,k} \to \cdots \to s_{i,n_i} \to \widehat{\Xi}_{i,n_i} \to u_i$ for $i = 1,\ldots,N$, $k = 3,\ldots,n_i-1$;

Remark 6: In line with [31], [32], and [33], Theorem 1 provides a practical consensus tracking result (i.e., convergence to a residual set). This is expected since [36] has proven that even for a single high-order system, asymptotic tracking is in general not possible (cf. Examples 2.1 and 2.2 of [36]).

Remark 7: The size of Ω_3 can be made small by increasing $c_{i,k}$, $\beta_{i,k}$, $\sigma_{i,k}$, $\rho_{i,k}$, and $\varrho_{i,k}$, and meanwhile decreasing $\zeta_{i,k}$, $b_{i,k}$, and γ_i for $i = 1,\ldots,N$, $k = 1,\ldots,n_i$. Then, the design parameters $c_{i,k}$, $\sigma_{i,k}$, $\beta_{i,k}$, $\zeta_{i,k}$, γ_i, $b_{i,k}$, and $\Theta_{i,k}$ can be adjusted so as to satisfy $\chi/\overline{\alpha} \le \varpi$, namely, $V(t) \le \varpi$ holds for $\forall t \ge 0$ due to the fact that $V(0) < \varpi$ and $\dot{V} \le 0$ when $V = \varpi$.

Remark 8: Even though the exact bound of $||\boldsymbol{\delta}||_2$ cannot be obtained due to the unknown constant $\Xi_{i,k}$ coming from the optimal weight vector of approximator, one can follow similar ideas as [46, Sec. 2.2] and [47, Sec. 4] and give an estimate for the upper bound of $||\boldsymbol{\delta}||_2$ by assuming $\Xi_{i,k}$ to be bounded by a known constant. A similar approach is adopted in the simulations of Section V-B. Fig. 8.

Remark 9: It is noted that the continuous function $F_{i,1}$ in (15) also embeds the effect of graph connectivity, since $F_{i,1}$ depends on the connectivity matrix $a_{i,j}$. At the same time, because the RBF NN activation functions depend on the neighboring states, one can rely on standard results [48] to get that any continuous function can be approximated by a RBF NN with desired accuracy over a compact set as long as we select enough neural network nodes. Similar idea is used in [23, eq. (18)], [24, eq. (12)], and [32, eq. (20)] to approximate unknown system nonlinearities over compact sets.

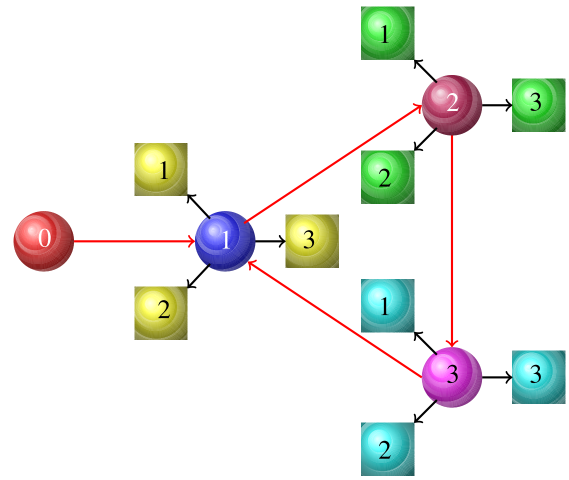

Fig. 1. Communication graph between leader 0 and follower agents 1, 2, and 3. Each agent can switch among three dynamics, represented as three squares around each agent.

Remark 10: Because the universal approximation ability of RBF NNs is valid only for a compact set, Theorem 1 has used invariant set theory to prove that Ω_0 is an invariant set where all closed-loop signals are retained all the time. The effectiveness of the adopted approximators has also been validated in the simulation (cf. Section V-A. Fig. 5).

Remark 11: Despite the dimension of input variable $\boldsymbol{Z}_{i,k}$ in activation function $\boldsymbol{\phi}_{i,k}(\boldsymbol{Z}_{i,k})$ inevitably grows as subsystem order k grows, there are two solutions to handle this issue: one is to use the fact $||\boldsymbol{\phi}_{i,k}(\boldsymbol{Z}_{i,k})|| \le ||\boldsymbol{\phi}_{i,k}(\bar{\boldsymbol{Z}}_{i,k})||$ to reduce the dimension of $\boldsymbol{Z}_{i,k}$ during the control design and stability analysis as done in [24, Lemma 1 and eq. (13)] and [49, Lemma 4 and eq. (15)], where $\dim(\bar{\boldsymbol{Z}}_{i,k}) < \dim(\boldsymbol{Z}_{i,k})$. Another one is to bound $||\boldsymbol{\phi}_{i,k}(\boldsymbol{Z}_{i,k})||$ as $||\boldsymbol{\phi}_{i,k}(\boldsymbol{Z}_{i,k})|| \le \Theta_{i,k}$ as done in [32, Lemma 3], [33, Lemma 2] and in our article [cf. (17)], where $\Theta_{i,k} > 0$ is an appropriately chosen constant.

V. Simulation Examples

A. Numerical Example

To validate the effectiveness of the proposed scheme, one leader (labeled by 0) with three follower agents are considered with the directed graph in Fig. 1.

The odd powers are taken as $r_{1,1} = 3$, $r_{1,2} = 5$, $r_{2,1} = 3$, $r_{2,2} = 7$, $r_{3,1} = 5$, $r_{3,2} = 9$, $n_i = 2$, $i = 1,2,3$. For each follower, the switching signal is $\sigma_i(\cdot)$: $[0,\infty) \to \mathcal{M}_i = \{1,2,3\}$, which is shown in Fig. 2. Note that each follower has its own switching signal, and thus can switch asynchronously with respect to the other followers. The unknown switched nonlinearities $\varphi_{i,k}^{\sigma_i(t)}(\cdot)$ and $h_{i,k}^{\sigma_i(t)}(\cdot)$ are taken to be heterogeneous:

For follower agent 1, the three switching dynamics are:

$$\begin{aligned}
\varphi_{1,1}^1 &= 1.3 - \cos(x_{1,1}), & h_{1,1}^1 &= |\tanh(x_{1,1}^3)| + 1.6,\\
\varphi_{1,1}^2 &= 0.6 + \exp(-x_{1,1}^2), & h_{1,1}^2 &= \cos(x_{1,1}^3) + 2,\\
\varphi_{1,1}^3 &= 0.8 + 0.2\cos(x_{1,1}^3), & h_{1,1}^3 &= 2\cos(x_{1,1}^2),\\
\varphi_{1,2}^1 &= x_{1,2}x_{1,1} + 0.75, & h_{1,2}^1 &= 2(|\cos(x_{1,2}^2)| + 1.3),\\
\varphi_{1,2}^2 &= 0.7 + 0.2x_{1,2}^2, & h_{1,2}^2 &= 3\sin(x_{1,2}^2) + 4,\\
\varphi_{1,2}^3 &= \cos(x_{1,2}^2) + 0.3, & h_{1,2}^3 &= 5|\sin(0.1x_{1,2})| + 1.5.
\end{aligned}$$

TABLE I

PERFORMANCE INDICES FOR TRACKING ERRORS $s_{1,1}$, $s_{2,1}$, AND $s_{3,1}$ UNDER THREE SCHEMES

Tracking Error	Index	Proposed Method	Ref. [32]	Ref. [33]
$s_{1,1}$	ITAE	3.268	12.693	15.226
	RMSE	0.213	0.876	0.926
	MAE	0.031	0.127	0.139
$s_{2,1}$	ITAE	3.747	13.214	14.944
	RMSE	0.237	0.914	0.954
	MAE	0.024	0.096	0.126
$s_{3,1}$	ITAE	3.994	13.693	15.696
	RMSE	0.264	0.887	0.969
	MAE	0.0289	0.133	0.152

TABLE II

PERFORMANCE INDICES FOR CONTROL INPUTS u_1, u_2, AND u_3 UNDER THREE SCHEMES

Control Input	Index	Proposed Method	Ref. [32]	Ref. [33]
u_1	MACA	2.113	11.021	6.564
u_2	MACA	2.457	8.689	8.012
u_3	MACA	2.754	7.254	8.367

For follower agent 2, the three switching dynamics are:

$$
\begin{aligned}
\varphi_{2,1}^1 &= 1.1x_{2,1} + x_{2,1}^2, & h_{2,1}^1 &= 3\cos(x_{2,1}^2) + 5,\\
\varphi_{2,1}^2 &= x_{2,1}^2 + 0.5, & h_{2,1}^2 &= \sin(x_{2,1}^3) + 3,\\
\varphi_{2,1}^3 &= x_{2,1}^3 + 1.25, & h_{2,1}^3 &= \cos(x_{2,1}^2 + x_{2,1}^3) + 3,\\
\varphi_{2,2}^1 &= 0.5x_{2,2}^2 + 0.75, & h_{2,2}^1 &= 3 + 2\cos(\chi_{2,1}^3\chi_{2,2}),\\
\varphi_{2,2}^2 &= 1.3x_{2,1}^3 + 0.8x_{2,2}, & h_{2,2}^2 &= 2\cos(\chi_{2,1}^2) + 4,\\
\varphi_{2,2}^3 &= \cos(x_{2,1})x_{2,2} + 0.25, & h_{2,2}^3 &= 3\cos(x_{2,2}^3) + 5.
\end{aligned}
$$

For follower agent 3, the three switching dynamics are:

$$
\begin{aligned}
\varphi_{3,1}^1 &= 1.5\sin(x_{3,1}) + x_{3,1}^3, & h_{3,1}^1 &= |\sin(x_{3,1})| + 6,\\
\varphi_{3,1}^2 &= 0.3x_{3,1}^2 + \sin(x_{3,1}), & h_{3,1}^2 &= |\sin(x_{3,1}^3)| + 3,\\
\varphi_{3,1}^3 &= x_{3,1} + 0.2\cos(x_{3,1}), & h_{3,1}^3 &= \cos(x_{3,1}^2 + x_{3,1}^3) + 4.5,\\
\varphi_{3,2}^1 &= 0.5x_{3,1}^2 + 0.5x_{3,2}, & h_{3,2}^1 &= \cos(x_{3,2}^2) + 2,\\
\varphi_{3,2}^2 &= x_{3,2} + 0.8\sin(x_{3,1}), & h_{3,2}^2 &= 4\cos(x_{3,1}) + 5.5,\\
\varphi_{3,2}^3 &= \cos(x_{3,2}^2) + 0.7, & h_{3,2}^3 &= \cos(x_{3,2}^2) + 3.5.
\end{aligned}
$$

The leader output is $y_r(t) = 2\sin(t) + 2\sin(0.5t)$. For comparison purposes, three schemes are considered, the method proposed here and the two state-of-the-art methods of [32] and [33]. In our simulation, the centers and widths of RBF NNs are chosen on a regular lattice in the respective compact sets. In particular, the neural networks used to approximate $F_{1,1}(\mathbf{Z}_{1,1})$, $F_{2,1}(\mathbf{Z}_{2,1})$, and $F_{3,1}(\mathbf{Z}_{3,1})$, respectively, contain 27 (Case I) or 3 (Case II) nodes with centers evenly spaced in the interval $[-2.5, 2.5] \times [-2.5, 2.5] \times [-2.5, 2.5]$ and widths equal to two. The neural networks used to approximate $F_{1,2}(\mathbf{Z}_{1,2})$, $F_{2,2}(\mathbf{Z}_{2,2})$, and $F_{3,2}(\mathbf{Z}_{3,2})$, respectively, contain 64 (Case I) or 6 (Case II) nodes with centers evenly spaced in the interval $[-4, 4] \times [-4, 4] \times [-4, 4] \times [-4, 4] \times [-4, 4] \times [-4, 4] \times [-4, 4] \times [-4, 4] \times [-4, 4]$ and widths equal to two. The initial conditions for the follower agents are taken as: $x_{1,1}(0) = 0.5$, $x_{2,1}(0) = 0.55$, $x_{3,1}(0) = 0.75$, $x_{1,2}(0) = 0.25$, $x_{2,2}(0) = 1.5$, $x_{3,2}(0) = -0.75$, $\widehat{\Xi}_{1,1}(0) = \widehat{\Xi}_{1,2}(0) = 5$, $\widehat{\Xi}_{2,1}(0) = \widehat{\Xi}_{2,2}(0) = 7$, and $\widehat{\Xi}_{3,1}(0) = \widehat{\Xi}_{3,2}(0) = 10$. The design parameters are chosen to be: $c_{1,1} = 1.5$, $c_{2,1} = 2.5$, $c_{3,1} = 3$, $c_{1,2} = 1$, $c_{2,2} = 2$, $c_{3,2} = 1.5$, $\beta_{1,2} = \beta_{2,2} = \beta_{3,2} = 1$, $\beta_{1,1} = 7.5$, $\beta_{2,1} = 5$, $\beta_{3,1} = 15$, $\sigma_{1,1} = 0.25$, $\sigma_{2,1} = 0.75$, $\sigma_{3,1} = 0.5$, $\sigma_{1,2} = \sigma_{2,2} = \sigma_{3,2} = 1$, $\zeta_{1,1} = \zeta_{2,1} = \zeta_{3,1} = 0.5$, $\zeta_{1,2} = \zeta_{2,2} = \zeta_{3,2} = 0.75$, $b_{1,1} = b_{2,1} = b_{3,1} = 0.5$, $b_{1,2} = b_{2,2} = b_{3,2} = 1$, $\Theta_{1,1} = \Theta_{2,1} = \Theta_{3,1} = 5$, and $\Theta_{1,2} = \Theta_{2,2} = \Theta_{3,2} = 5\sqrt{5}$. The simulation results in Figs. 3 and 4 and in Tables I and II are carried out based on Case I. Tables I and II report the integral time absolute error (ITAE) $= [\int_0^T t|s_{i,1}(t)|dt]$, root mean square error (RMSE) $= [(1/T)\int_0^T s_{i,1}^2(t)dt]^{(1/2)}$, mean absolute error (MAE) $= [(1/T)|s_{i,1}(t)|dt]$, and mean absolute control actions (MACA) $= [(1/T)\int_0^T |u_i|]$ for $i = 1, 2, 3$, respectively. Fig. 2 reveals that the switching signals $\sigma_i(\cdot)$, $i = 1, 2, 3$, for three followers are asynchronous. It can be seen from Fig. 3 and Table I that the proposed method achieves smaller tracking errors $s_{1,1}$, $s_{2,1}$, and $s_{3,1}$ than that of [32] and [33]. From Fig. 4 and Table II, one can conclude that the proposed method exhibits smaller control actions than that of [32] and [33]. Fig. 5 shows that

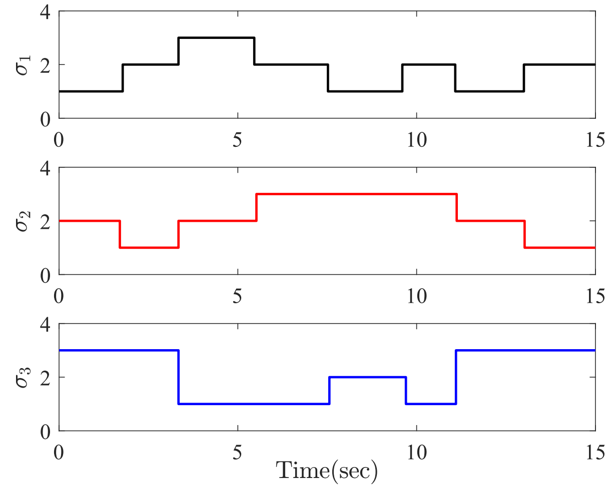

Fig. 2. Switching signals $\sigma_i(t)$ for the three followers. Note that the followers can switch asynchronously with each other.

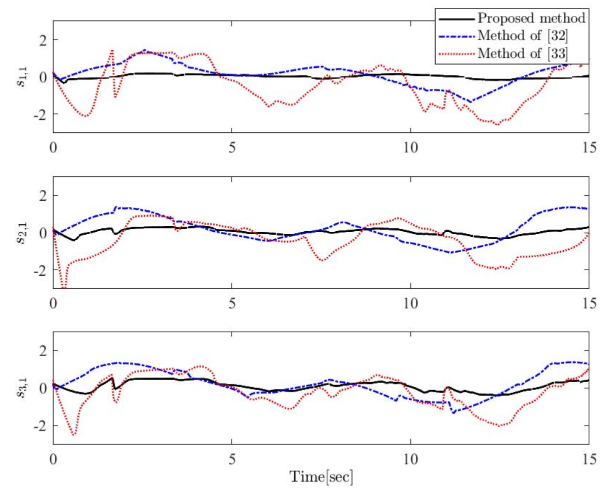

Fig. 3. Tracking errors $s_{1,1}$, $s_{2,1}$, and $s_{3,1}$ under three schemes.

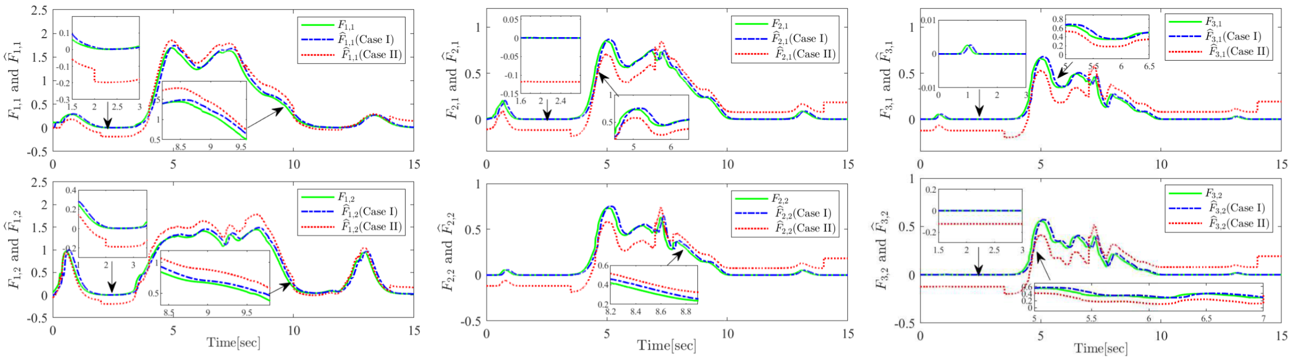

Fig. 4. Control inputs u_1, u_2, and u_3 under three schemes. The proposed scheme avoids high control gains, as the result of the reduced-complexity design (cf. Remark 5).

TABLE III

VALUES OF m_1, m_2, k_s, AND k_ω OF 10 FOLLOWERS

Agents	Mode	m_1(kg)	m_2(kg)	k_s(N/m^3)	k_ω(N/m)	Agents	Mode	m_1(kg)	m_2(kg)	k_s(N/m^3)	k_ω(N/m)
Follower 1	①	1.25	1.50	75	70	Follower 6	①	1.75	2.50	65	57
	②	1.80	1.75	70	85		②	1.95	2.75	75	60
	③	2.25	3.50	45	50		③	2.80	3.75	80	75
Follower 2	①	2.50	4.50	55	60	Follower 7	①	2.95	3.75	55	67
	②	2.00	4.80	80	75		②	1.50	2.45	75	85
	③	1.85	2.75	45	50		③	2.25	1.85	55	60
Follower 3	①	1.50	2.35	45	55	Follower 8	①	2.85	3.75	60	75
	②	1.95	4.25	50	60		②	2.50	2.75	65	80
	③	2.25	3.50	70	55		③	1.85	2.55	70	65
Follower 4	①	2.75	3.50	75	70	Follower 9	①	2.25	3.75	65	70
	②	1.80	4.75	55	65		②	1.50	2.80	75	70
	③	2.65	4.50	80	75		③	2.25	3.65	80	75
Follower 5	①	3.25	2.75	75	55	Follower 10	①	1.75	2.85	65	55
	②	2.85	3.50	70	60		②	3.25	1.75	60	65
	③	3.50	4.00	65	70		③	1.85	3.50	65	75

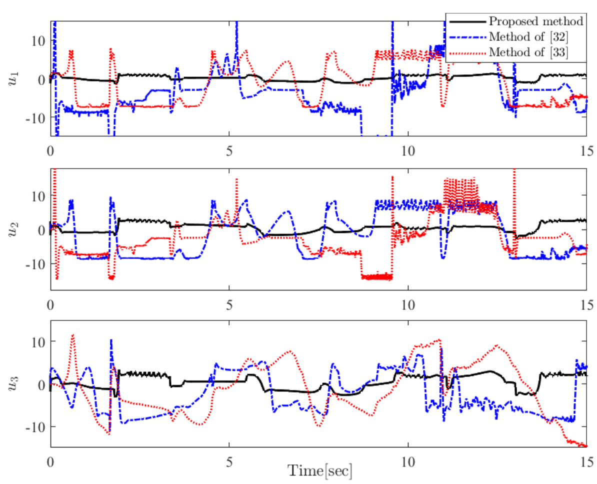

Fig. 5. True (unknown) $F_{1,1}$, $F_{1,2}$, $F_{2,1}$, $F_{2,2}$, $F_{3,1}$, $F_{3,2}$, and their NN approximations $\widehat{F}_{1,1}$, $\widehat{F}_{1,2}$, $\widehat{F}_{2,1}$, $\widehat{F}_{2,2}$, $\widehat{F}_{3,1}$, $\widehat{F}_{3,2}$.

the RBF NN approximators can achieve satisfactory approximation performances as long as we choose a sufficiently large number of network nodes.

B. Practical Example

To further validate the developed method, a multiagent version of the underactuated weakly coupled mechanical benchmark in [36] is considered, also shown in Fig. 6. The system includes a mass $m_{i,1}^{\sigma_i}$ on a horizontal smooth surface and an inverted pendulum $m_{i,2}^{\sigma_i}$ supported by a massless rod. The mass is connected to the wall surface by a linear spring and to the inverted pendulum by a nonlinear spring with a cubic force deformation relation. The dynamics of the ith agent can be represented by

$$\begin{cases} \ddot{\theta}_i = \dfrac{g\sin(\theta_i)}{l} + \dfrac{k_{i,s}^{\sigma_i(t)}}{m_{i,2}^{\sigma_i(t)} l}\big(x_i - l\sin(\theta_i)\big)^3\cos(\theta_i), \\ \ddot{x}_i = -\dfrac{k_{i,\omega}^{\sigma_i(t)}}{m_{i,1}^{\sigma_i(t)}}x_i - \dfrac{k_{i,s}^{\sigma_i(t)}}{m_{i,1}^{\sigma_i(t)}}\big(x_i - l\sin(\theta_i)\big)^3 + \dfrac{u_i}{m_{i,1}^{\sigma_i(t)}} \end{cases} \tag{44}$$

for $i = 1, \ldots, 10$, and $\sigma_i(\cdot) : [0, +\infty) \to \mathcal{M}_i=\{1, 2, \ldots, 10\}$, where $\theta_i \in (-(\pi/2), (\pi/2))$, x_i is the displacement of $m_{i,1}^{\sigma_i(t)}$, u_i is the control force acting on $m_{i,1}^{\sigma_i(t)}$. Moreover, $k_{i,s}^{\sigma_i(t)}$ and $k_{i,\omega}^{\sigma_i(t)}$ are spring coefficients, and l is the pendulum length. The specific values of $m_{i,1}^{\sigma_i(t)}$, $m_{i,2}^{\sigma_i(t)}$, $k_{i,s}^{\sigma_i(t)}$, and $k_{i,\omega}^{\sigma_i(t)}$, $i = 1, \ldots, 10$, are given in the Table III, and the switching signal is given in Fig. 7. The following change of coordinates:

$$x_{i,1} = \theta_i, \quad x_{i,2} = \dot{\theta}_i, \quad x_{i,3} = x_i, \quad x_{i,4} = \dot{x}_i \tag{45}$$

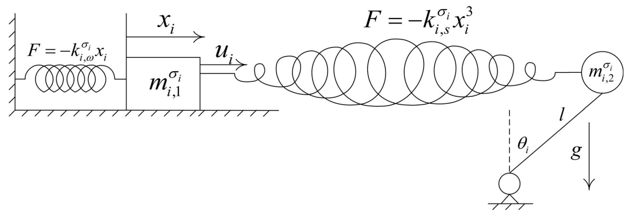

Fig. 6. Underactuated weakly coupled mechanical system.

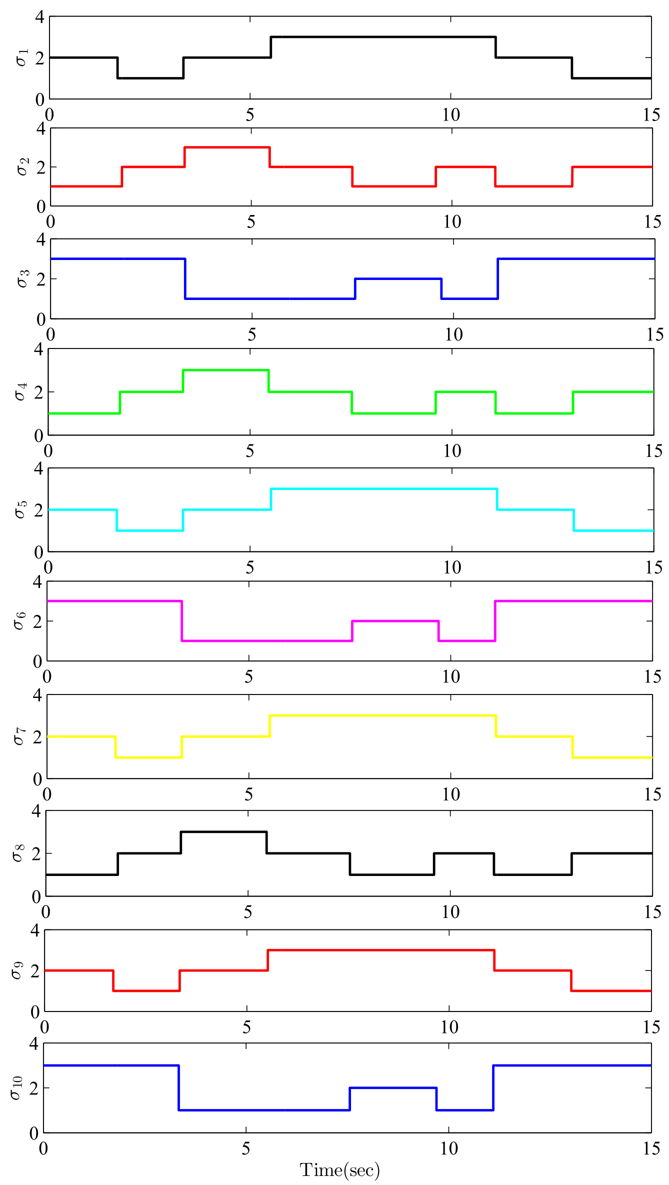

Fig. 7. Asynchronous switching signal $\sigma_i(t)$.

transform (44) into

$$\begin{cases}\dot{x}_{i,1}=x_{i,2},\ \dot{x}_{i,2}=\varphi_{i,2}^{\sigma_i(t)}(\bar{\boldsymbol{x}}_{i,2})+h_{i,2}^{\sigma_i(t)}(\bar{\boldsymbol{x}}_{i,2})x_{i,3}^3,\\ \dot{x}_{i,3}=x_{i,4},\ \dot{x}_{i,4}=\varphi_{i,4}^{\sigma_i(t)}(\bar{\boldsymbol{x}}_{i,4})+h_{i,4}^{\sigma_i(t)}(\bar{\boldsymbol{x}}_{i,4})u_i\end{cases}\tag{46}$$

where $\varphi_{i,2}^{\sigma_i(t)}(\bar{\boldsymbol{x}}_{i,2}) = (g/l)\sin(x_{i,1}) + (k_{i,s}^{\sigma_i(t)}/m_{i,2}^{\sigma_i(t)}l)\cos(x_{i,1})[3x_{i,3}l^2\times\sin^2(x_{i,1})-3x_{i,3}^2 l\sin(x_{i,1})-l^3\times\sin^3(x_{i,1})]$, $\varphi_{i,4}(\bar{\boldsymbol{x}}_{i,4}) = -(k_{i,\omega}^{\sigma_i(t)}/m_{i,1}^{\sigma_i(t)})x_{i,3} - (k_{i,s}^{\sigma_i(t)}/m_{i,1}^{\sigma_i(t)})[x_{i,3}^3 - l^3\sin^3(x_{i,1}) - 3x_{i,3}^2 l\sin(x_{i,1}) + 3x_{i,3}l^2\sin^2(x_{i,1})]$, $h_{i,2}^{\sigma_i(t)}(\bar{\boldsymbol{x}}_{i,2}) = (k_{i,s}^{\sigma_i(t)}/m_{i,2}^{\sigma_i(t)}l)\cos(x_{i,1})$, and $h_{i,4}^{\sigma_i(t)}(\bar{\boldsymbol{x}}_{i,4})=(1/m_{i,1}^{\sigma_i(t)})$.

The leader signal is the same as Example A. Due to space limits, we do not repeat all the state-of-the-art comparisons as in the previous example. The neural networks used to approximate $F_{i,1}(\boldsymbol{Z}_{i,1})$ and $F_{i,2}(\boldsymbol{Z}_{i,2})$ for $i=1,\ldots,10$ contain 27 nodes with centers evenly spaced in the interval $[-2.5,2.5]\times[-2.5,2.5]\times[-2.5,2.5]$ and widths equal to two. The neural networks used to approximate $F_{i,3}(\boldsymbol{Z}_{i,3})$ and $F_{i,4}(\boldsymbol{Z}_{i,4})$ for $i=1,\ldots,10$ contain 81 nodes with centers evenly spaced in the interval $[-4,4]\times[-4,4]\times[-4,4]\times[-4,4]\times[-4,4]\times[-4,4]\times[-4,4]\times[-4,4]\times[-4,4]\times[-4,4]$ and widths equal to two. The initial conditions for the follower agents are taken as: $x_{i,1}(0)=0$ for $i=1,\ldots,7$, $x_{i,1}(0)=0.15$ for $i=8,9,10$, $x_{i,2}(0)=0.25$ for $i=1,\ldots,5$, $x_{i,2}(0)=-0.5$ for $i=6,\ldots,10$, $x_{i,3}(0)=0$ for $i=1,\ldots,10$, $x_{i,4}(0)=-0.75$ for $i=1,\ldots,6$, $x_{i,4}(0)=0.25$ for $i=7,\ldots,10$, $\widehat{\Xi}_{i,1}(0)=\widehat{\Xi}_{i,2}(0)=5$ for $i=1,\ldots,5$, and $\widehat{\Xi}_{i,3}(0)=\widehat{\Xi}_{i,4}(0)=7.5$ for $i=6,\ldots,10$. The design parameters are chosen to be: $c_{i,1}=1.5$ for $i=1,\ldots,4$, $c_{i,1}=2.5$ for $i=5,\ldots,10$, $c_{i,2}=c_{i,3}=2$ for $i=1,\ldots,10$, $c_{i,4}=3.5$ for $i=1,\ldots,10$, $\beta_{i,1}=5.5$ for $i=1,\ldots,10$, $\beta_{i,2}=7$ for $i=1,\ldots,10$, $\beta_{i,3}=\beta_{i,4}=3.5$ for $i=1,\ldots,10$, $\sigma_{i,1}=\sigma_{i,2}=0.5$ for $i=1,\ldots,10$, $\sigma_{i,3}=\sigma_{i,4}=0.75$ for $i=1,\ldots,10$, $\zeta_{i,1}=\zeta_{i,3}=0.25$ for $i=1,\ldots,10$, $\zeta_{i,2}=\zeta_{i,4}=0.5$ for $i=1,\ldots,10$, $b_{i,1}=b_{i,2}=b_{i,3}=b_{i,4}=1$ for $i=1,\ldots,10$, $\Theta_{i,1}=5$, and $\Theta_{i,2}=\Theta_{i,3}=\Theta_{i,4}=7\sqrt{5}$ for $i=1,\ldots,10$. Fig. 8(a) shows that the 10 followers track the leader signal with bounded tracking errors. Fig. 8(b) depicts the evolution of control inputs. Fig. 8(c) draws the curves of $||\boldsymbol{\delta}||_2$ as well as its theoretical bound which is calculated assuming $\Xi_{i,k}$ to be bounded as $\Xi_{i,k}\le 7\sqrt{5}$ for $i=1,\ldots,10$ and $k=1,\ldots,4$.

VI. Conclusion

This article proposed a result about distributed consensus tracking for high-order nonlinear multiagent systems with switched dynamics. The distinguishing feature of the proposed design is a new separation-based lemma that can simplify the control design in a twofold sense: the complexity of the virtual and actual control laws is sensibly reduced; the power of the control gains does not increase exponentially with the order of the subsystems.

Appendix

Proof of Proposition 1: When x_1 is not equal to zero, we let $x_2=px_1$, $p\in\mathbf{R}$. Thus, using (ii) yields

$$|\digamma(x_1)(\digamma(\overline{p})-1)|\le\overline{\upsilon}(d)|\digamma(p)|\cdot|\digamma(x_1)|+|\digamma(x_1)|d\tag{47}$$

where $\overline{p}=p+1$. Applying (i) on both sides of (47) gives

$$|\digamma(x_1+x_2)-\digamma(x_1)|\le M+|\digamma(x_1)|d\tag{48}$$

where $M=\overline{\upsilon}(d)|\digamma(x_2)|$. At this point, two situations are considered:

Situation 1: when $\digamma(x_1)<0$, it follows from (48) that:

$$\overline{d}\digamma(x_1)-M\le\digamma(x_1+x_2)\le\underline{d}\digamma(x_1)+M\tag{49}$$

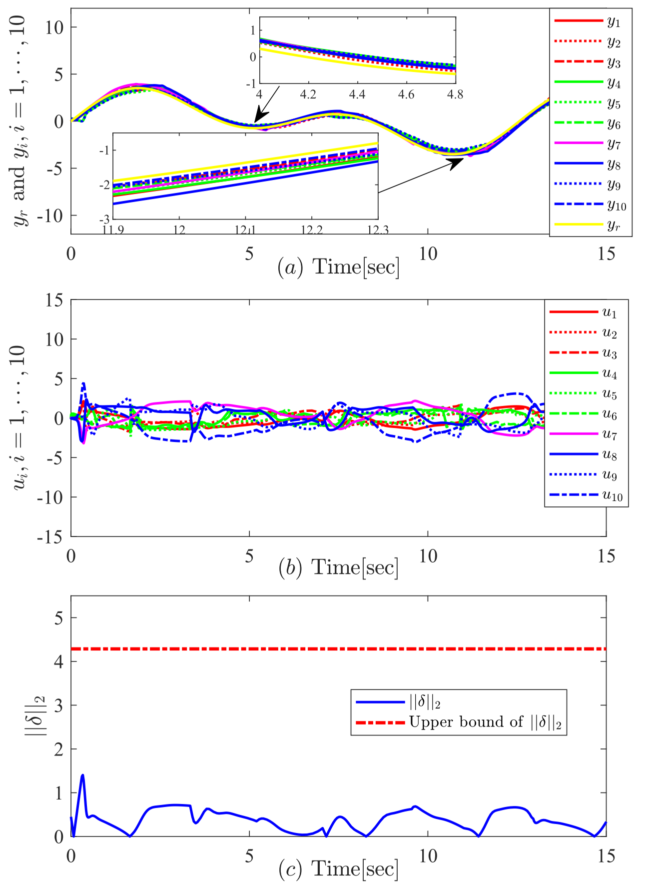

Fig. 8. (a) Follower outputs y_i (i=1,…,10) and leader output y_r. (b) Control inputs. (c) Norm of consensus tracking error $||\delta||_2$ and its theoretic bound.

where $\overline{d} = d + 1$ and $\underline{d} = 1 - d$.

Situation 2: when $F(x_1) \geq 0$, one has

$$\underline{d}F(x_1) - M \leq F(x_1 + x_2) \leq \overline{d}F(x_1) + M. \tag{50}$$

When x_1 is equal to zero, (4) becomes

$$F(x_2) = \ell(x_1, x_2)F(0) + \upsilon(x_1, x_2)F(x_2) \tag{51}$$

which we have to prove. Using (1), we get $F(0) = F(0)F(x_2)$ and (51) becomes $F(x_2) = \left[\ell(0, x_2)F(0) + \upsilon(0, x_2)\right]F(x_2)$ which holds by taking $\ell(0, x_2) \equiv 0$ and $\upsilon(0, x_2) \equiv 1$. This completes the proof. ∎

Proof of Lemma 3: We will verify that condition (2) in Lemma 3 holds (condition (1) is trivially satisfied). Using the binomial theorem [50, Sec. 3.1, page. 10] leads to

$$\overline{p}^r = 1 + \frac{p \cdot r!}{(r-1)!} + \cdots + \frac{p^{r-1} \cdot r!}{(r-1)!} + p^r \tag{52}$$

which further results in

$$|\overline{p}^r - 1| \leq \sum_{k=1}^{r} \frac{r!}{k!(r-k)!}|p|^k. \tag{53}$$

At this point, it is noted that for any positive constant d taking value in $(0, 1)$, we select an appropriately small constant $l > 0$ satisfying $d = \sum_{k=1}^{r}(r!/k!(r-k)!)(r-k/r)l^{(r/r-k)}$. In the meantime, if we choose $\overline{\upsilon}(d) = \sum_{k=1}^{r}(r!/k!(r-k)!)(k/r)l^{-(r/k)}$, then, it follows from Lemma 1 that $d + \overline{\upsilon}(d)|p^r| = \sum_{k=1}^{r}[(r!/k!(r-k)!)(k/r)l^{-(r/k)}|p|^r + (r!/k!(r-k)!)(r-k/r)l^{(r/r-k)}] \geq \sum_{k=1}^{r}(r!/k!(r-k)!) \times |p|^k$, which combined with (53) gives $|\overline{p}^r - 1| \leq d + \overline{\upsilon}(d)|p^r|$. Therefore, $F(z) = z^r$ is a separable function according to Proposition 1. This completes the proof. ∎

Finally, the proof of Proposition 1 reveals that, if we let $z = x_1 + x_2$, then, it holds that $(x_1 + x_2)^r = \ell(x_1, x_2)x_1^r + \upsilon(x_1, x_2)x_2^r$, where $\ell(x_1, x_2) \in [\underline{\ell}_1, \overline{\ell}_1]$ with $\underline{\ell}_1 = 1 - d$ and $\overline{\ell}_1 = 1 + d$, and $|\upsilon(x_1, x_2)| \leq \overline{\upsilon}(d)$.

Proof of Theorem 1: It follows from (40) that:

$$\dot{V}_{i,n_i} \leq -\alpha_i V_{i,n_i} + \Gamma_i$$

where $\alpha_i = \min\{(r_i - r_{i,k} + 2)\zeta_{i,k}, \beta_{i,k}\sigma_{i,k} : 1 \leq k \leq n_i\}$ with $\zeta_{i,k} = \gamma_i^{(r_{i,k}-1)/(r_i+1)}(c_{i,k} - \theta_{i,k} - \vartheta_{i,k-1})$ and $\Gamma_i = \sum_{k=1}^{n_i}[(1/2)\sigma_{i,k}\Xi_{i,k}^2 + \hbar_{i,k} + \gamma_i(c_{i,k} - \theta_{i,k} - \vartheta_{i,k-1})]$. Therefore, the derivative of V can be obtained as

$$\dot{V} \leq -\overline{\alpha}V + \chi \tag{54}$$

where $\overline{\alpha} = \min_{1\leq i\leq N}\{\alpha_i\}$ and $\chi = \sum_{i=1}^{N}\Gamma_i$. It can be concluded from (54) that $(\chi/\overline{\alpha})$ can be made arbitrarily small by increasing $c_{i,k}$, $\beta_{i,k}$, $\sigma_{i,k}$, $\rho_{i,k}$, and $\varrho_{i,k}$, and meanwhile decreasing $\zeta_{i,k}$, $b_{i,k}$, and γ_i for $i = 1, \ldots, N$, $k = 1, \ldots, n_i$. Namely, it is possible to make $(\chi/\overline{\alpha}) \leq \varpi$ by selecting the design parameters appropriately. Then, in light of (54), we have that $\dot{V} \leq 0$ holds true for $V = \varpi$: consequently, the compact set Ω_0 is an invariant set and all closed-loop signals stay inside of the compact set Ω_0 all the time since $V(0) < \varpi$.

A bound on the tracking error can be obtained as follows: integrating $\dot{V}(t)$ on $[0, t]$ gives

$$\int_0^t \mathrm{d}\left[\exp(\overline{\alpha}t)V(t)\right] \leq \int_0^t \chi \exp(\overline{\alpha}t)\ \mathrm{d}t \tag{55}$$

which suggests that

$$V(t) \leq \left(V(0) - \frac{\chi}{\overline{\alpha}}\right)\exp(-\overline{\alpha}t) + \frac{\chi}{\overline{\alpha}} \leq V(0) + \frac{\chi}{\overline{\alpha}}. \tag{56}$$

Thus, invoking (16) yields that $\lim_{t\to+\infty}(s_{i,1}^{r_i - r_{i,1}+2}/r_i - r_{i,1} + 2) \leq (\chi/\overline{\alpha})$, which further leads to

$$\lim_{t\to+\infty}\|s_1\| \leq \sqrt{\sum_{i=1}^{N}\left[\left(\frac{\chi}{\overline{\alpha}}\overline{\psi}_i\right)^2\right]^{\frac{1}{\psi_i}}}. \tag{57}$$

Then, from the inequalities below (5), one gets that $\lim_{t\to+\infty}\|\boldsymbol{\delta}\| \leq (\Gamma/\underline{\lambda}_{\min}(\overline{\mathscr{L}} + \mathscr{B}))$. This concludes the proof. ∎

REFERENCES

[1] K. K. Oh, M. C. Park, and H. S. Ahn, "A survey of multi-agent formation control," *Automatica*, vol. 53, pp. 424–440, Mar. 2015.

[2] W. Ren and Y. Cao, *Distributed Coordination of Multi-Agent Networks: Emergent Problems, Models, and Issues*. London, U.K.: Springer-Verlag, 2010.

[3] W. Yu, G. Wen, G. Chen, and J. Cao, *Distributed Cooperative Control of Multi-agent Systems*, 1st ed. Hoboken, NJ, USA: Wiley, 2017.

[4] Y. Song and Y. Wang, *Cooperative Control of Nonlinear Networked Systems: Infinite-Time and Finite-Time Design Methods*. Springer, 2019. [Online]. Available: https://www.springer.com/gp/book/9783030049713

[5] X. Jin, "Adaptive iterative learning control for high-order nonlinear multi-agent systems consensus tracking," *Syst. Control Lett.*, vol. 89, pp. 16–23, Mar. 2016.

[6] A. Das and F. L. Lewis, "Distributed adaptive control for synchronization of unknown nonlinear networked systems," *Automatica*, vol. 46, no. 12, pp. 2014–2021, Dec. 2010.

[7] Q. Shen, P. Shi, J. Zhu, S. Wang, and Y. Shi, "Neural networks-based distributed adaptive control of nonlinear multiagent systems," *IEEE Trans. Neural Netw. Learn. Syst.*, vol. 31, no. 3, pp. 1010–1021, Mar. 2020.

[8] C. L. P. Chen, G.-X. Wen, Y.-J. Liu, and F.-Y. Wang, "Adaptive consensus control for a class of nonlinear multiagent time-delay systems using neural networks," *IEEE Trans. Neural Netw. Learn. Syst.*, vol. 25, no. 6, pp. 1217–1226, Jun. 2014.

[9] W. Zou, P. Shi, Z. Xiang, and Y. Shi, "Consensus tracking control of switched stochastic nonlinear multiagent systems via event-triggered strategy," *IEEE Trans. Neural Netw. Learn. Syst.*, vol. 31, no. 3, pp. 1036–1045, Mar. 2020.

[10] G. Dong, H. Li, H. Ma, and R. Lu, "Finite-time consensus tracking neural network FTC of multi-agent systems," *IEEE Trans. Neural Netw. Learn. Syst.*, vol. 32, no. 2, pp. 653–662, Feb. 2021, doi: 10.1109/TNNLS.2020.2978898.

[11] W. Zou, P. Shi, Z. Xiang, and Y. Shi, "Finite-time consensus of second-order switched nonlinear multi-agent systems," *IEEE Trans. Neural Netw. Learn. Syst.*, vol. 31, no. 5, pp. 1757–1762, May 2020, doi: 10.1109/TNNLS.2019.2920880.

[12] J. Xu, "Nonrepetitive leader–follower formation tracking for multiagent systems with LOS range and angle constraints using iterative learning control," *IEEE Trans. Cybern.*, vol. 49, no. 5, pp. 1748–1758, May 2019.

[13] S. El-Ferik, A. Qureshi, and F. L. Lewis, "Neuro-adaptive cooperative tracking control of unknown higher-order affine nonlinear systems," *Automatica*, vol. 50, no. 3, pp. 798–808, Mar. 2014.

[14] W. Meng, Q. Yang, S. Jagannathan, and Y. Sun, "Distributed control of high-order nonlinear input constrained multiagent systems using a backstepping-free method," *IEEE Trans. Cybern.*, vol. 49, no. 11, pp. 3923–3933, Nov. 2019.

[15] W. Wang and S. Tong, "Adaptive fuzzy bounded control for consensus of multiple strict-feedback nonlinear systems," *IEEE Trans. Cybern.*, vol. 48, no. 2, pp. 522–531, Feb. 2018.

[16] Q. Shen and P. Shi, "Distributed command filtered backstepping consensus tracking control of nonlinear multiple-agent systems in strict-feedback form," *Automatica*, vol. 53, pp. 120–124, Mar. 2015.

[17] Y. Wang and Y. Song, "Leader-following control of high-order multi-agent systems under directed graphs: Pre-specified finite time approach," *Automatica*, vol. 87, pp. 113–120, Jan. 2018.

[18] C.-C. Hua, X. You, and X.-P. Guan, "Leader-following consensus for a class of high-order nonlinear multi-agent systems," *Automatica*, vol. 73, pp. 138–144, Nov. 2016.

[19] W. Wang, C. Wen, and J. Huang, "Distributed adaptive asymptotically consensus tracking control of nonlinear multi-agent systems with unknown parameters and uncertain disturbances," *Automatica*, vol. 77, pp. 133–142, Mar. 2017.

[20] W. Yu, W. Ren, W. X. Zheng, G. Chen, and J. Lü, "Distributed control gains design for consensus in multi-agent systems with second-order nonlinear dynamics," *Automatica*, vol. 49, no. 7, pp. 2107–2115, Jul. 2013.

[21] J. Xu, "Fault tolerant finite-time leader–follower formation control for autonomous surface vessels with LOS range and angle constraints," *Automatica*, vol. 68, pp. 228–236, Jun. 2016.

[22] Y. Wang and Y. Song, "Fraction dynamic-surface-based neuroadaptive finite-time containment control of multiagent systems in nonaffine pure-feedback form," *IEEE Trans. Neural Netw. Learn. Syst.*, vol. 28, no. 3, pp. 678–689, Mar. 2017.

[23] S. J. Yoo, "Distributed consensus tracking of a class of asynchronously switched nonlinear multi-agent systems," *Automatica*, vol. 87, pp. 421–427, Jan. 2018.

[24] W. Meng, P. X. Liu, Q. Yang, and Y. Sun, "Distributed synchronization control of nonaffine multiagent systems with guaranteed performance," *IEEE Trans. Neural Netw. Learn. Syst.*, vol. 31, no. 5, pp. 1571–1580, May 2020, doi: 10.1109/TNNLS.2019.2920892.

[25] S. Yoo, "Distributed low-complexity fault-tolerant consensus tracking of switched uncertain nonlinear pure-feedback multi-agent systems under asynchronous switching," *Nonlinear Anal.: Hybrid Syst.*, vol. 32, pp. 239–253, May 2019.

[26] M. Krstic, I. Kanellakopoulos, and P. Kokotovic, *Nonlinear and Adaptive Control Design*. New York, NY, USA: Wiley, 1995.

[27] C. Qian and W. Lin, "Output feedback control of a class of nonlinear systems: A nonseparation principle paradigm," *IEEE Trans. Autom. Control*, vol. 47, no. 10, pp. 1710–1715, Oct. 2002.

[28] W. Lin and C. Qian, "Adding one power integrator: A tool for global stabilization of high-order lower-triangular systems," *Syst. Control Lett.*, vol. 39, no. 5, pp. 339–351, Apr. 2000.

[29] W. Lin and R. Pongvuthithum, "Adaptive output tracking of inherently nonlinear systems with nonlinear parameterization," *IEEE Trans. Autom. Control*, vol. 48, no. 10, pp. 1737–1749, Oct. 2003.

[30] M. Lv, W. Yu, J. Cao, and S. Baldi, "Consensus in high-power multiagent systems with mixed unknown control directions via hybrid nussbaum-based control," *IEEE Trans. Cybern.*, early access, Nov. 4, 2020, doi: 10.1109/TCYB.2020.3028171.

[31] X. Zhao, X. Wang, G. Zong, and X. Zheng, "Adaptive neural tracking control for switched high-order stochastic nonlinear systems," *IEEE Trans. Cybern.*, vol. 47, no. 10, pp. 3088–3099, Oct. 2017.

[32] C. Shi, Z. Liu, X. Dong, and Y. Chen, "A novel error-compensation control for a class of high-order nonlinear systems with input delay," *IEEE Trans. Neural Netw. Learn. Syst.*, vol. 29, no. 9, pp. 4077–4087, Sep. 2018.

[33] X. D. Zhao, P. Shi, X. L. Zheng, and J. H. Zhang, "Intelligent tracking control for a class of uncertain high-order nonlinear systems," *IEEE Trans. Neural Netw. Learn. Syst.*, vol. 27, no. 9, pp. 1976–1982, Sep. 2016.

[34] N. Wang, G. Wen, Y. Wang, F. Zhang, and A. Zemouche, "Fuzzy adaptive cooperative consensus tracking of high-order nonlinear multiagent networks with guaranteed performances," *IEEE Trans. Cybern.*, early access, Feb. 26, 2021, doi: 10.1109/TCYB.2021.3051002.

[35] N. Wang, Y. Wang, G. Wen, M. Lv, and F. Zhang, "Fuzzy adaptive constrained consensus tracking of high-order multi-agent networks: A new event-triggered mechanism," *IEEE Trans. Syst., Man, Cybern. Syst.*, under review.

[36] C. Qian and W. Lin, "Practical output tracking of nonlinear systems with uncontrollable unstable linearization," *IEEE Trans. Autom. Control*, vol. 47, no. 1, pp. 21–36, Jan. 2002.

[37] M. Lv, B. De Schutter, W. Yu, W. Zhang, and S. Baldi, "Nonlinear systems with uncertain periodically disturbed control gain functions: Adaptive fuzzy control with invariance properties," *IEEE Trans. Fuzzy Syst.*, vol. 28, no. 4, pp. 746–757, Apr. 2020.

[38] M. Lv, S. Baldi, and Z. Liu, "The non-smoothness problem in disturbance observer design: A set-invariance-based adaptive fuzzy control method," *IEEE Trans. Fuzzy Syst.*, vol. 27, no. 3, pp. 598–604, Mar. 2019.

[39] M. Lv, W. Yu, and S. Baldi, "The set-invariance paradigm in fuzzy adaptive DSC design of large-scale nonlinear input-constrained systems," *IEEE Trans. Syst., Man, Cybern., Syst.*, vol. 51, no. 2, pp. 1035–1045, Feb. 2021.

[40] X. Wang, H. Li, G. Zong, and X. Zhao, "Adaptive fuzzy tracking control for a class of high-order switched uncertain nonlinear systems," *J. Franklin Inst.*, vol. 354, no. 15, pp. 6567–6587, Oct. 2017.

[41] W. Lin, R. Pongvuthithum, and C. Qian, "Control of high-order nonholonomic systems in power chained form using discontinuous feedback," *IEEE Trans. Autom. Control*, vol. 47, no. 1, pp. 108–115, Jan. 2002.

[42] H. Zhang and F. L. Lewis, "Adaptive cooperative tracking control of higher-order nonlinear systems with unknown dynamics," *Automatica*, vol. 48, no. 7, pp. 1432–1439, Jul. 2012.

[43] P. Ioannou and J. Sun, *Robust Adaptive Control*. New York, NY, USA: Dover, 2012.

[44] B. Jiang, Q. Shen, and P. Shi, "Neural-networked adaptive tracking control for switched nonlinear pure-feedback systems under arbitrary switching," *Automatica*, vol. 61, pp. 119–125, Nov. 2015.

[45] Y. P. Hong and C.-T. Pan, "A lower bound for the smallest singular value," *Linear Algebra Appl.*, vol. 172, pp. 27–32, Jul. 1992.

[46] W. Meng, Q. Yang, S. Jagannathan, and Y. Sun, "Adaptive neural control of high-order uncertain nonaffine systems: A transformation to affine systems approach," *Automatica*, vol. 50, no. 5, pp. 1473–1480, May 2014.

[47] J. Na, X. Ren, and D. Zheng, "Adaptive control for nonlinear pure-feedback systems with high-order sliding mode observer," *IEEE Trans. Neural Netw. Learn. Syst.*, vol. 24, no. 3, pp. 370–382, Mar. 2013.

[48] R. M. Sanner and J.-J.-E. Slotine, "Gaussian networks for direct adaptive control," *IEEE Trans. Neural Netw.*, vol. 3, no. 6, pp. 837–863, Nov. 1992.

[49] F. Wang, B. Chen, C. Lin, and X. Li, "Distributed adaptive neural control for stochastic nonlinear multiagent systems," *IEEE Trans. Cybern.*, vol. 47, no. 7, pp. 1795–1803, Jul. 2017.

[50] M. Abramowitz and I. A. Stegun, *Handbook of Mathematical Functions With Formulas, Graphs, and Mathematical Tables*, 9th ed. New York, NY, USA: Dover, 1972.

Maolong Lv received the B.Sc. degree in electrical engineering and automation and the M.Sc. degree in control science and engineering from Air Force Engineering University, Xi'an, China, in 2014 and 2016, respectively. He is currently pursuing the Ph.D. degree in systems and control with the Delft Center for Systems and Control, Delft University of Technology, Delft, The Netherlands.

His research interests include nonlinear control, adaptive learning control, deep reinforcement learning, swarm control and switched systems with applications in networked control, multiagent systems and hypersonic vehicles. In 2018 he was awarded a Descartes Excellence Fellowship from the Institut Français des Pays-Bas, which allowed him a research visit and a cooperation with the University of Grenoble, Grenoble, France on the topic of adaptive networked systems with emphasis on ring stability analysis for mixed traffic with human-driven and autonomous vehicles from September 2018 to January 2019.

Wenwu Yu (Senior Member, IEEE) received the B.Sc. degree in information and computing science and the M.Sc. degree in applied mathematics from the Department of Mathematics, Southeast University, Nanjing, China, in 2004 and 2007, respectively, and the Ph.D. degree from the Department of Electronic Engineering, City University of Hong Kong, Hong Kong, in 2010.

He is currently the Founding Director of Laboratory of Cooperative Control of Complex Systems and the Deputy Associate Director of Jiangsu Provincial Key Laboratory of Networked Collective Intelligence, an Associate Dean with the School of Mathematics, and a Full Professor with the Endowed Chair Honor in Southeast University, Nanjing, China. He held several visiting positions in Australia, China, Germany, Italy, The Netherlands, and the USA. His research interests include multiagent systems, complex networks and systems, disturbance control, distributed optimization, machine learning, game theory, cyberspace security, smart grids, intelligent transportation systems, big-data analysis, etc.

Dr. Yu severs as an Editorial Board Member of several flag journals, including IEEE TRANSACTIONS ON CIRCUITS AND SYSTEMS II, IEEE TRANSACTIONS ON INDUSTRIAL INFORMATICS, IEEE TRANSACTIONS ON SYSTEMS, MAN, AND CYBERNETICS: SYSTEMS, *Science China Information Sciences*, *Science China Technological Sciences*, and so on. He was listed by Clarivate Analytics/Thomson Reuters Highly Cited Researchers in Engineering from 2014 to 2020. He publishes about 100 IEEE Transactions journal articles with more than 18000 citations. Moreover, he was a recipient of the Second Prize of State Natural Science Award of China in 2016.

Jinde Cao (Fellow, IEEE) received the B.S. degree from Anhui Normal University, Wuhu, China, the M.S. degree from Yunnan University, Kunming, China, and the Ph.D. degree from Sichuan University, Chengdu, China, all in mathematics/applied mathematics, in 1986, 1989, and 1998, respectively.

He is an Endowed Chair Professor, the Dean of the School of Mathematics, the Director of the Jiangsu Provincial Key Laboratory of Networked Collective Intelligence of China and the Director of the Research Center for Complex Systems and Network Sciences, Southeast University, Nanjing, China.

Prof. Cao was a recipient of the National Innovation Award of China, the Gold medal of Russian Academy of Natural Sciences, the Obada Prize and the Highly Cited Researcher Award in Engineering, Computer Science, and Mathematics by Thomson Reuters/Clarivate Analytics. He is elected as a member of the Academy of Europe, a Foreign Member of Russian Academy of Engineering, a member of the European Academy of Sciences and Arts, a Foreign Member of Russian Academy of Natural Sciences, a Foreign Fellow of Pakistan Academy of Sciences, a fellow of African Academy of Sciences, a foreign Member of the Lithuanian Academy of Sciences, an International Academy for Systems and Cybernetic Sciences (IASCYS) Academician, and a Full Member of Sigma Xi.

Simone Baldi (Senior Member, IEEE) received the B.Sc. degree in electrical engineering and the M.Sc. and Ph.D. degrees in automatic control systems engineering from the University of Florence, Florence, Italy, in 2005, 2007, and 2011, respectively.

He is currently a Professor with the School of Mathematics, Southeast University, Nanjing, China, with a guest position with the Delft Center for Systems and Control, Delft University of Technology, Delft, The Netherlands, where he was an Assistant Professor. His research interests include adaptive and switched systems with applications in networked control and multiagent systems.

Dr. Baldi was received the Outstanding Reviewer of *Applied Energy* in 2016, *Automatica* in 2017, and *IET Control Theory and Applications* in 2018. He is the Subject Editor of *International Journal of Adaptive Control and Signal Processing* and an Associate Editor of IEEE CONTROL SYSTEMS LETTERS.